# Tuning Plasmon Resonance of $In_2O_3$ Nanocrystals throughout Mid-Infrared: Dopant, Phase, and Electronic Structure Dependence

WATERLOO INSTITUTE FOR nanotechnology

WISE
WATERLOO INSTITUTE FOR SUSTAINABLE ENERGY

Radovanovic
RESEARCH GROUP


*Pavle V. Radovanović*

**Department of Chemistry**


UNIVERSITY OF WATERLOO
CONCORDIA CUM VERITATE

# Plasmonic Nanocrystals

- **The localized surface plasmon resonance (LSPR) is the result of the collective oscillation of conduction electrons in the particle upon interaction with light.**

- **The resonant conditions of the plasmon are sensitive to the surrounding medium – suitable applications as sensors, chemical probes, light concentrators in solar cells, surface-enhanced Raman spectroscopy (SERS)**

- **Gold and silver nanocrystals are most commonly used nanostructured plasmonic materials – easy to synthesize, relatively inert to oxidation and other reactions, have high carrier concentrations**

- **Issues with metal nanoparticles: high optical losses (due to electronic transitions), cost, inability to tune charge carriers**

- **Possibility of coupling plasmon and exciton in a single phase**

# Transparent Metal Oxides (TMOs)

- Combine transparency and conductivity (key functionalities that do not naturally stand together)

- Wide band gap (3.7 eV for $In_2O_3$)

- High charge carrier density and mobility (oxygen vacancy is the major donor which causes the n-type conductivity)

$$O_O^x \rightarrow V_O^{\bullet\bullet} + \frac{1}{2}O_2 + 2e^-$$

- Polymorphic – suitable for investigation of structure-function relationship. Exhibit a complex interplay among several active degrees of freedom (charge, lattice, orbital, and spin)

# Model System: $In_2O_3$

Bixbyite

**bcc-$In_2O_3$**

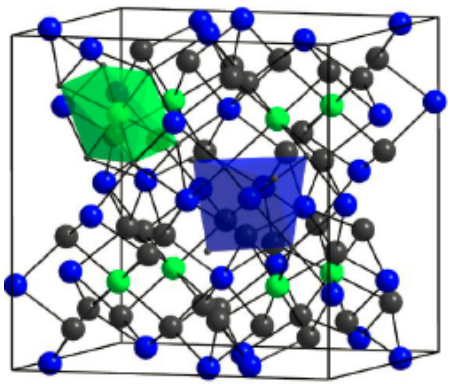

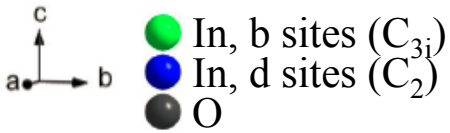


Corundum

**rh-$In_2O_3$**

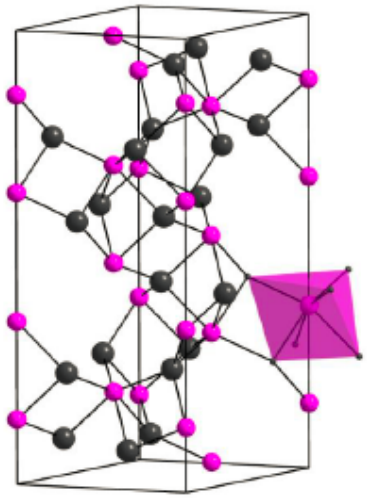


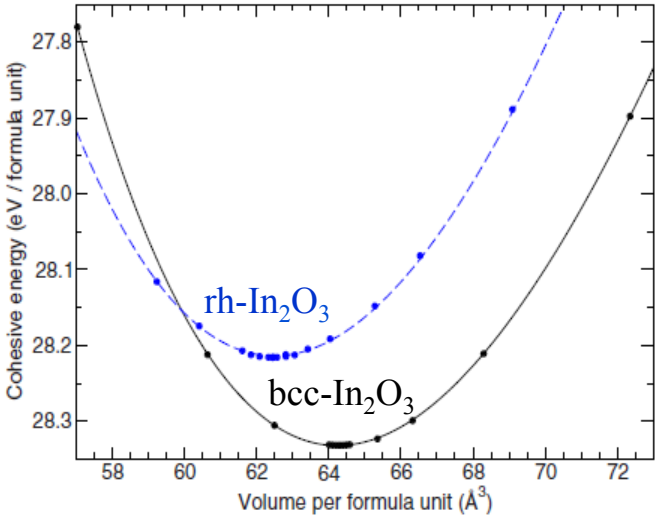


*Phys. Rev. B* **2008**, *77*, 155107

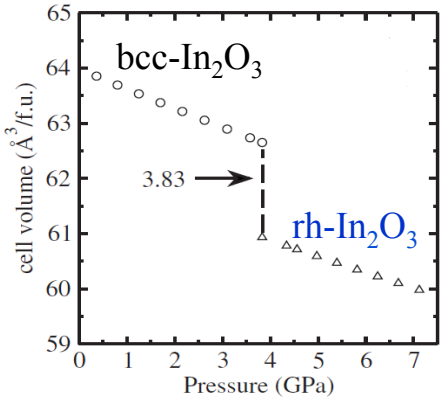


*Phys. Rev. B* **2007**, *76*, 075129

# Morphology and Phase Transformations

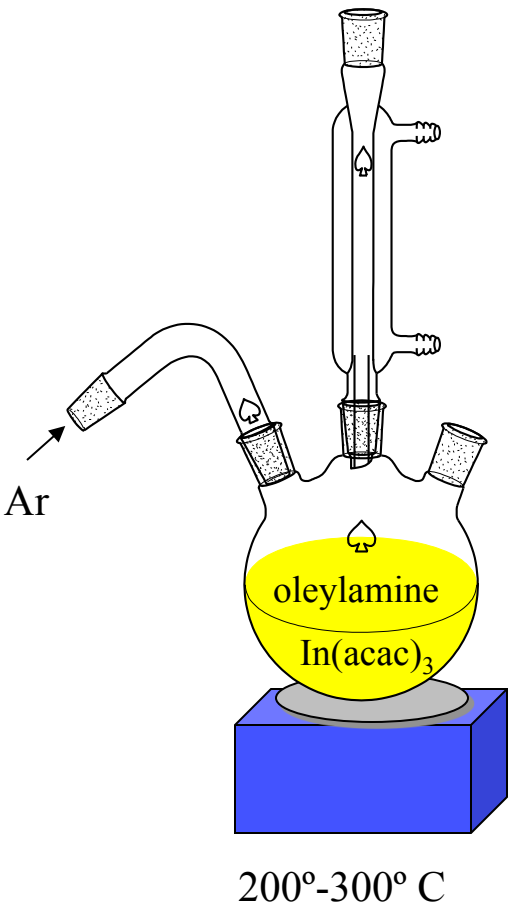


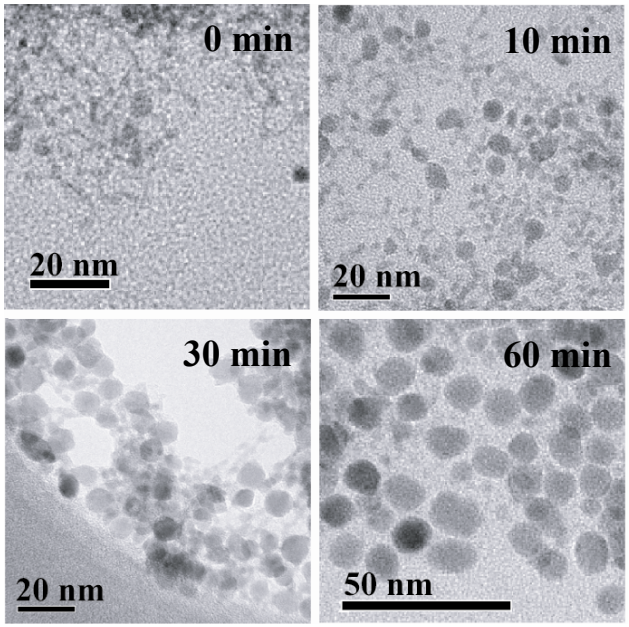


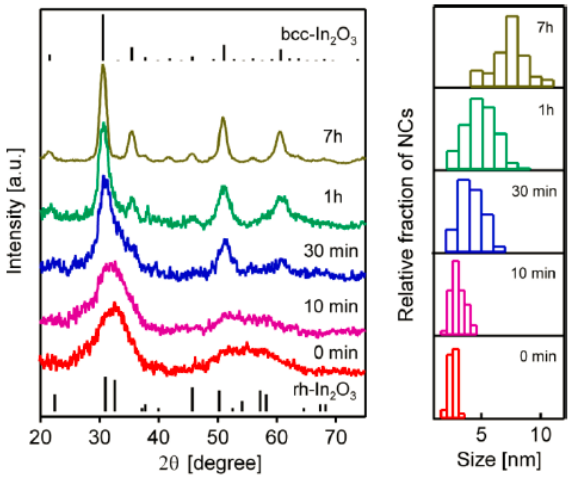


- Surface energy
- Surface stress (g)

- **Proposed mechanism: hydrolysis and dehydration cascade**

$$In^{3+} + 3OH^- \longrightarrow In(OH)_3 \xrightarrow{-H_2O} InOOH$$

$$2InOOH \xrightarrow{-H_2O} rh\text{-}In_2O_3 \longrightarrow bcc\text{-}In_2O_3$$

Farvid, S. S.; Dave, N.; Radovanovic, P. V. *Chem. Mater.* **2010**, *22*, 9-11.

# X-ray Absorption Spectroscopy as a Structural Tool

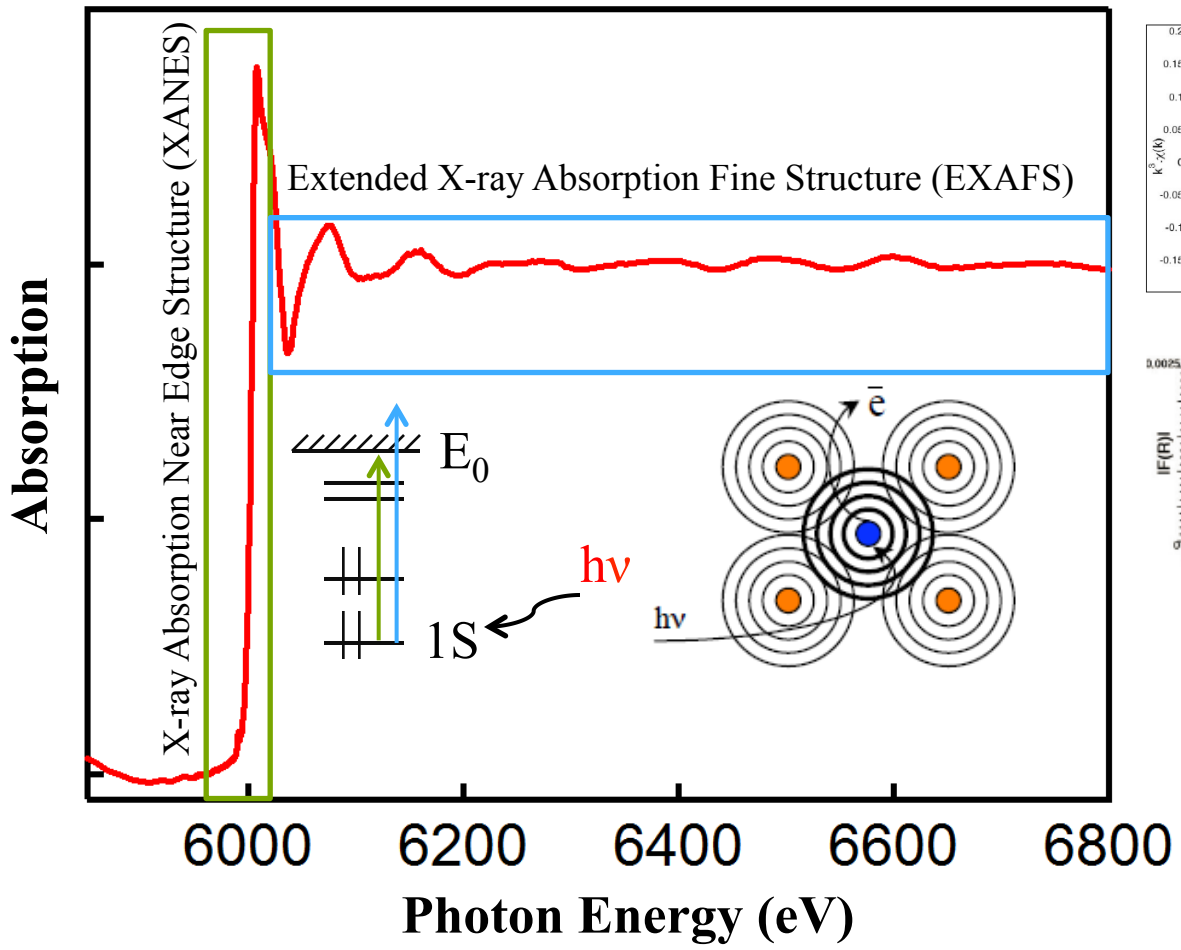


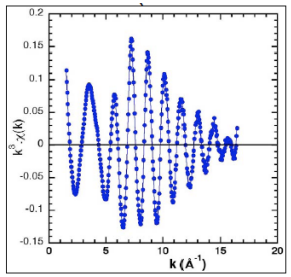


Fourier Transform

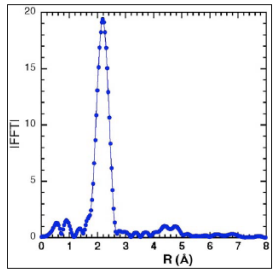


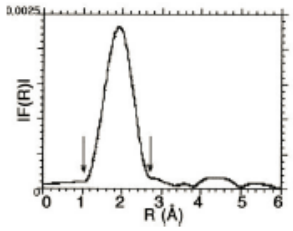


Back Fourier Transform

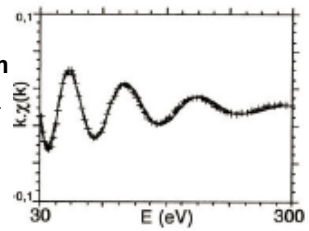


Provide information about the:

- Nature of neighbors
- Bond distance
- Number of neighbors

# Surface Stress Effects

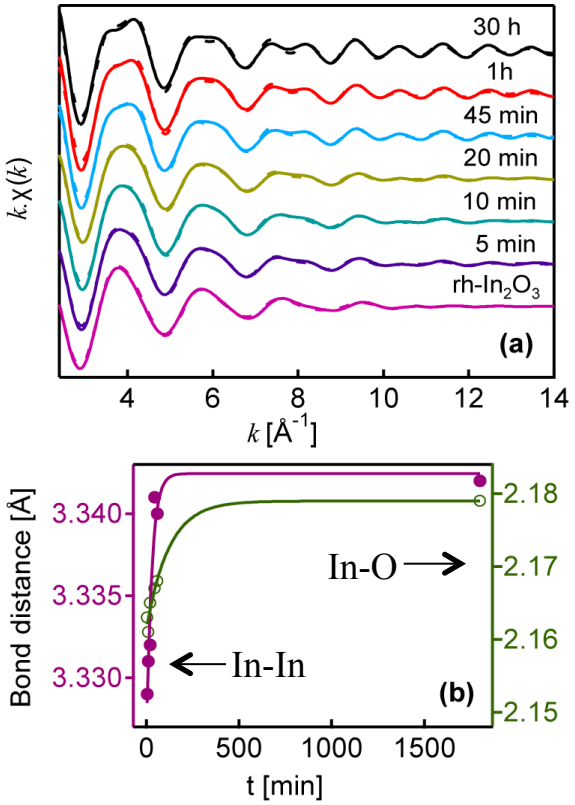


| | In-O | | | In-In$_1$ | | | |
|---|---|---|---|---|---|---|---|
| *t* (min) | *N* | *R* (Å) | $\sigma^{2\,a}$ (Å$^2$) | *N* | *R* (Å) | $\sigma^2$ (Å$^2$) | $\rho^b$ (%) |
| 5 | 6.0 | 2.163 | 0.007 | 3.3 | 3.329 | 0.010 | 0.6 |
| 10 | 6.0 | 2.161 | 0.006 | 3.8 | 3.331 | 0.012 | 0.6 |
| 20 | 6.0 | 2.165 | 0.007 | 3.2 | 3.332 | 0.009 | 0.5 |
| 45 | 6.0 | 2.167 | 0.006 | 5.1 | 3.341 | 0.008 | 1.3 |
| 60 | 6.0 | 2.168 | 0.005 | 5.9 | 3.340 | 0.008 | 2.0 |
| 1800 | 6.0 | 2.179 | 0.006 | 6.0 | 3.342 | 0.005 | 2.5 |

Increased surface stress ($g$) ⟶ Compressed In-O bonds
⟶ Average fractional decrease in atomic volume ($\Omega$)

$$\frac{\Delta\Omega}{\Omega_0} = \beta\frac{2g}{r} \leftrightarrow \Delta p = \frac{2g}{r}$$

Particle size <5nm ⟶ rh-$In_2O_3$

Farvid, S. S.; Radovanovic, P. V.
*J. Am. Chem. Soc.* **2012**, *134*, 7015.

# Mechanism of Phase Transformation

- Mechanisms of phase transformation can be identified via model fitting approach

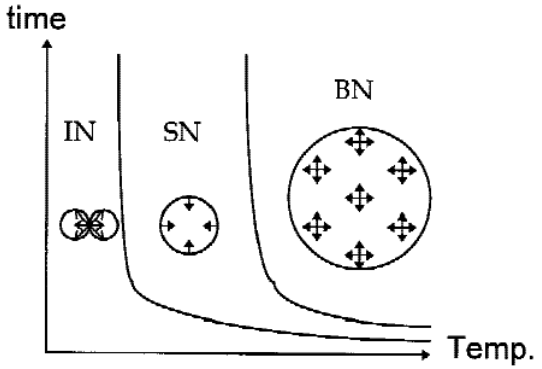


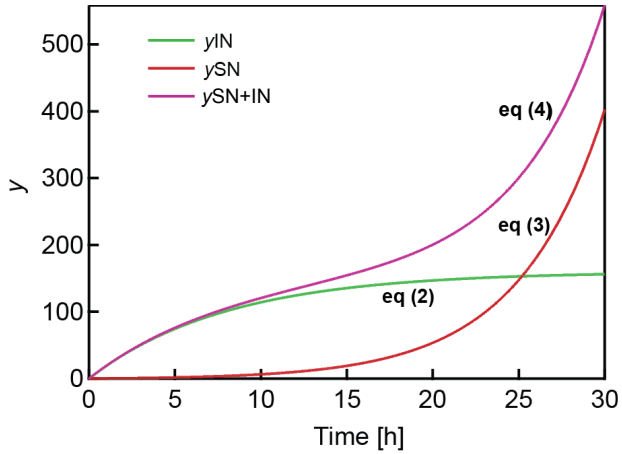


$$(1)\ y = \frac{(D_{rh}/D_o)^3}{(1-\alpha)} - 1$$

$$(2)\ y(\mathrm{IN}) = k_{IN} N_o t_x (1 - e^{t/t_x})$$

$$(3)\ y(\mathrm{SN}) = e^{k_{SN} t} - 1$$

$$(4)\ y(\mathrm{IN+SN}) = (1 + \frac{k_{IN} N_o}{k_{SN}})(e^{k_{SN} t} - 1)$$

$t$ is time
$t_x$ is the time at which IN function levels off
$k_{SN}$ is the SN rate constant
$k_{IN}$ is the IN rate constant
$N_o$ is the number of particles at time 0

Zhang, H.; Banfield, J. F. *J. Mater. Res.* **2000**, *15*, 437-448

# Kinetic Results

$$y = \frac{(D_{rh} / D_o)^3}{(1-\alpha)} - 1$$

- 1:20 precursor to solvent ratio shown below
- Increasing rate constant with increasing T also observed for other dilutions

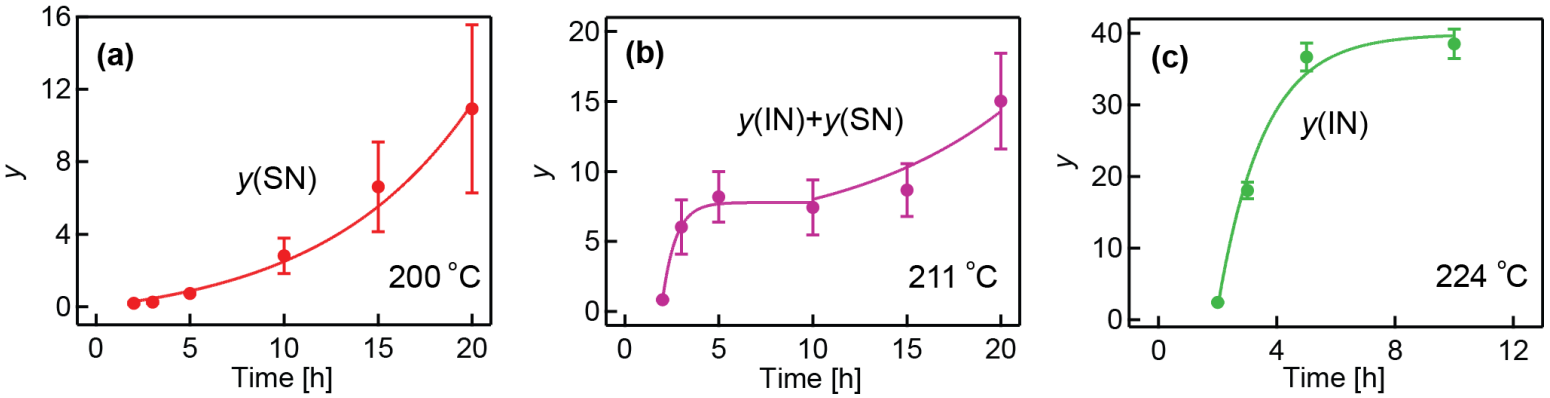


| Dilution | T [°C] | Model | $k_{SN}$ [h$^{-1}$] | $k_{IN}N_o$ [h$^{-1}$] |
|---|---|---|---|---|
| 1:20 | 200 | y(SN) | 0.1251 | |
| | 206 | y(SN) | 0.2149 | |
| | 215 | y(IN+SN) | 0.3359 | 1.086 |
| | 224 | y(IN) | | 23.58 |

# Activation Energy

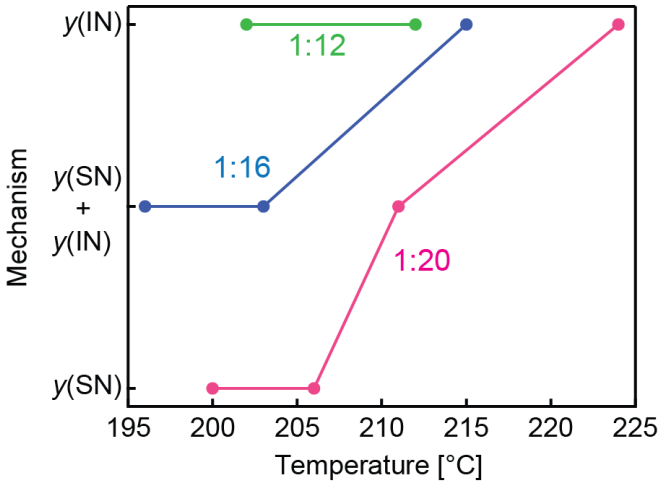


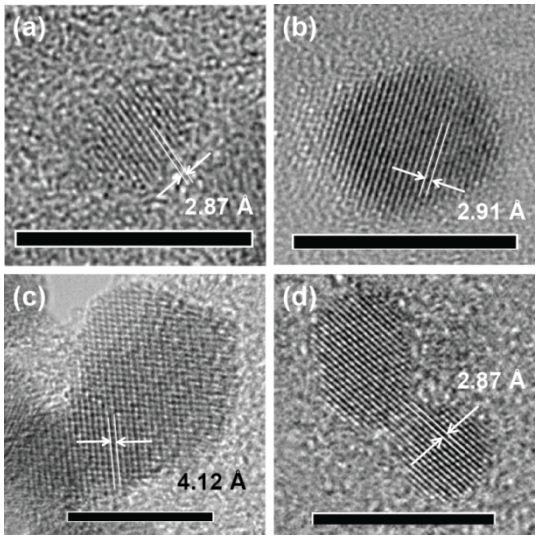


Scale bar in all images, 10 nm

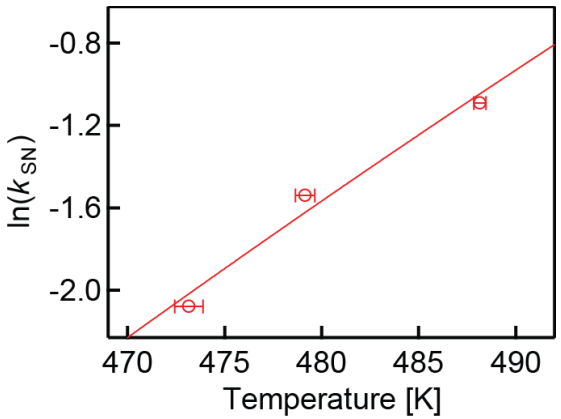


$$\ln(k) = \ln(A_o) - \frac{E_a}{RT}$$

- $E_a$(SN) is on average ca. 144 ± 30 kJ/mol
- $E_a$(IN) is on average ca. 152 ± 60 kJ/mol

Hutfluss, L. N.; Radovanovic, P. V. *J. Am. Chem. Soc.* **2015**, *137*, 1101-1108.

# Morphology and Phase Control

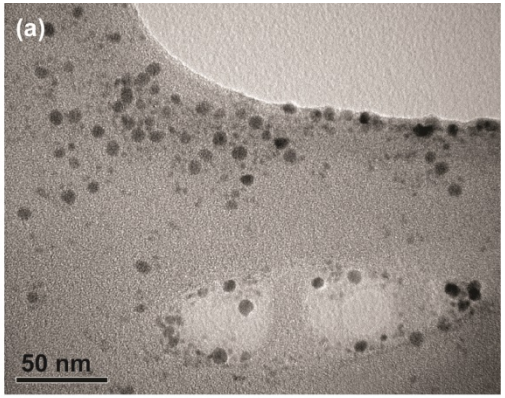


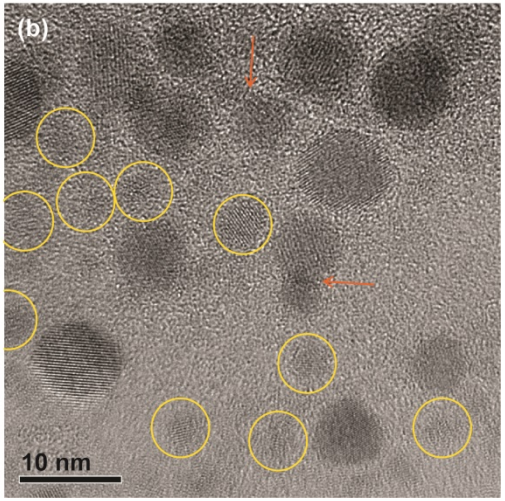


200 °C, 5h, 1:20 dilution

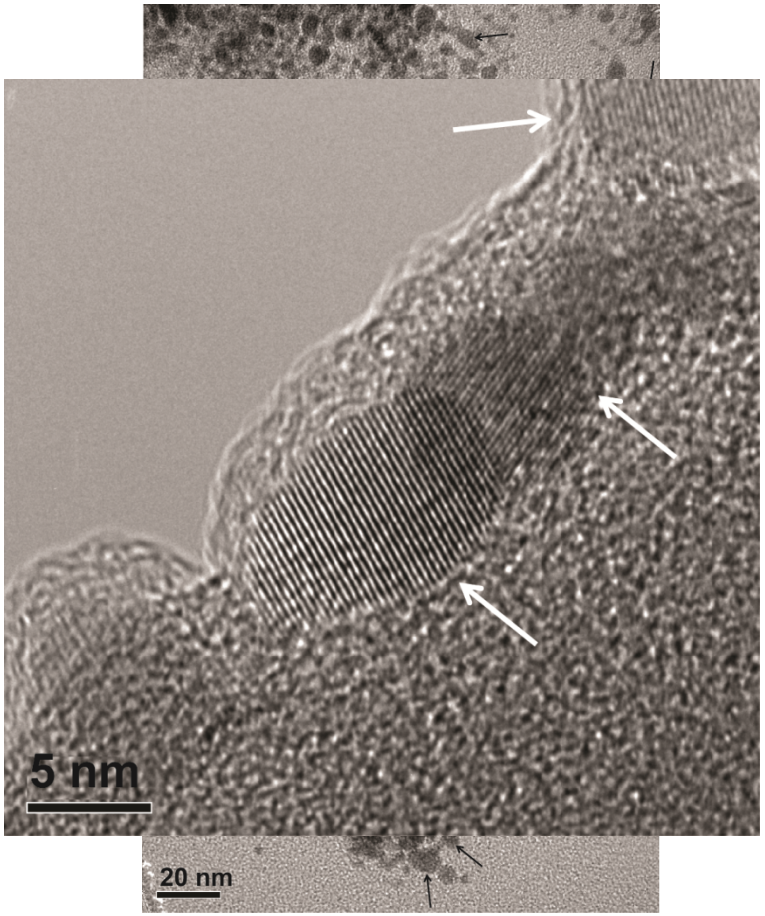


200 °C, 1h, 1:12 dilution

# Mechanism Summary: Molecular Analogy

- Illustrate the effects of precursor to solvent ratio **(a,b)** and temperature **(c,d)** on the mechanism of phase transformation
- IN dominates at high concentration, high T
- SN dominates at low concentration, low T

rh-$In_2O_3$ "conformation"

bcc-$In_2O_3$ "conformation"

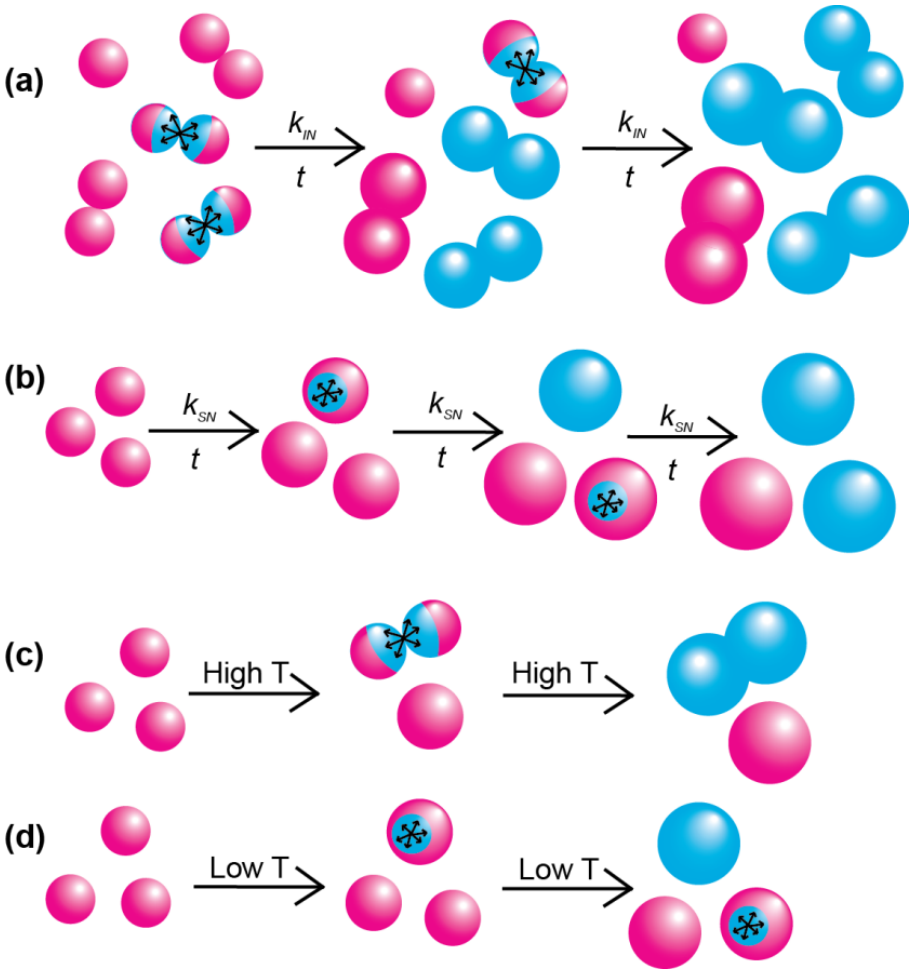


Hutfluss, L. N.; Radovanovic, P. V. *J. Am. Chem. Soc.* **2015**, *137*, 1101-1108.

# Phase-Controlled Synthesis of $In_2O_3$ NCs

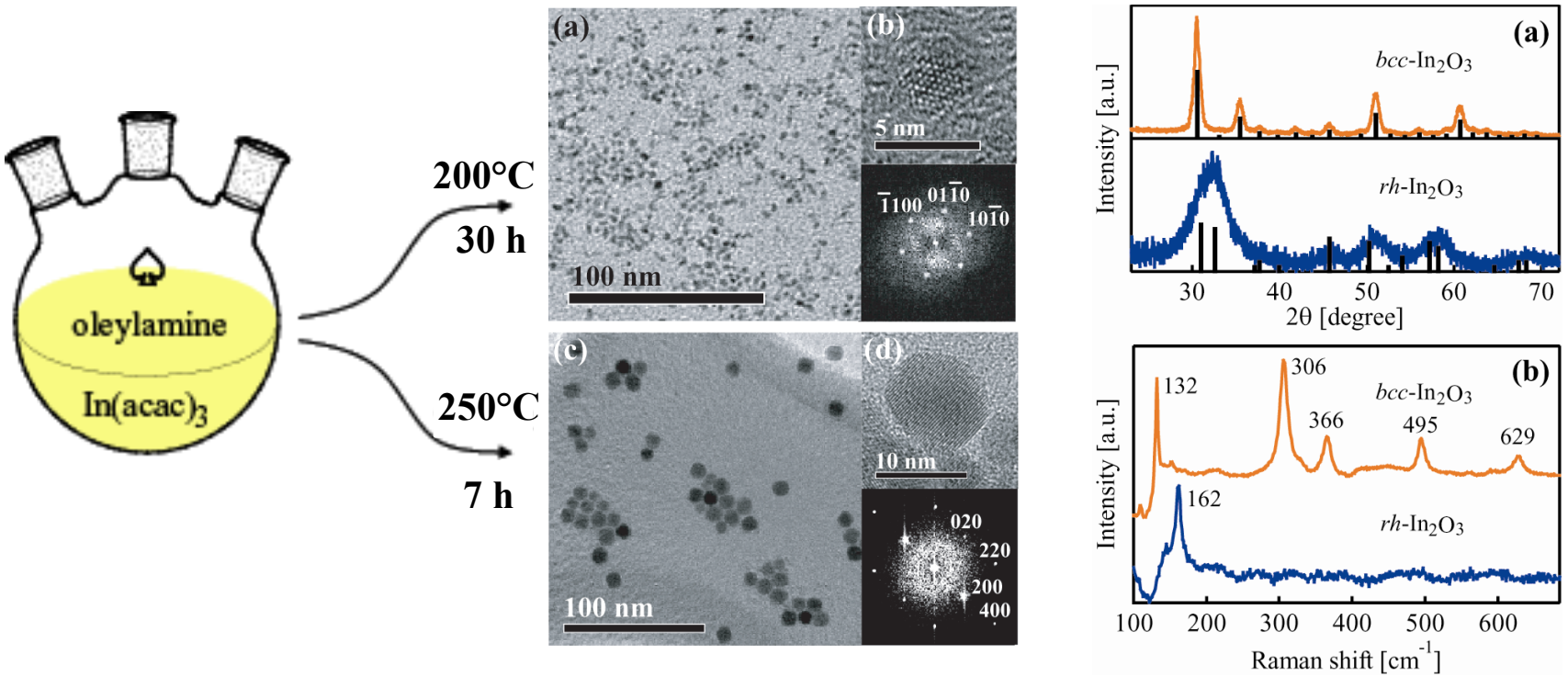


Farvid, S. S.; Dave, N.; Radovanovic, P. V. *Chem. Mater.* **2010**, *22*, 9-11.

# Why Does the NC Phase Matter?

- Controlling the electronic structure of metal oxide nanostructures
  - Transparency and conductivity (*Chem. Mater.* **2010**, *22*, 9-11; *J. Phys. Chem. C* **2011**, *115,* 406–413)
  - Anisotropy (*J. Phys. Chem. C* **2015**, *119,* 17450–17457)
  - Magnetic exchange interactions (*J. Am. Chem. Soc.* **2014**, *136*, 7669–7679; *Chem. Mater.* **2013**, *25*, 233-244)
- Controlling the electronic structure and formation of native defects
  - Size and composition tunable photoluminescence (*J. Am. Chem Soc.* **2010**, *132*, 9250-9252; *J. Am. Chem Soc.* **2011**, *133*, 6711-6719)
  - Understading defect interactions in reduced dimanstions (*J. Mater. Chem. C* **2014**, *2*, 3212-3222; *Appl. Phys. Lett.* **2012**, *100*, 141903; *Chem. Comm.*, **2011**,*47*, 7161-7163)
  - Energy efficient white light generation (*J. Am. Chem. Soc.* **2013**, *135*, 14520−14523; *J. Phys. Chem. C* **2015**, *119*, 5687-5696)

# Plasmonic Properties of Colloidal ITO NCs

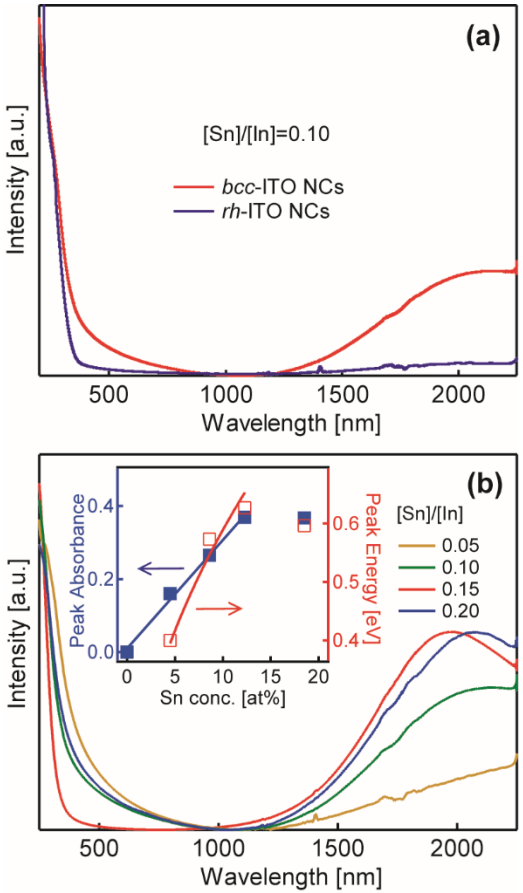


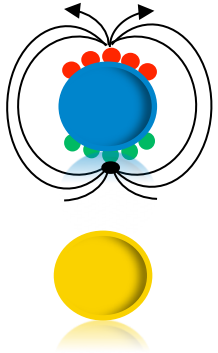

bcc-ITO

rh-ITO

## Drude-Lorentz Model

$$\alpha_{free-electrons} = \frac{Ne^2}{m^* \varepsilon_0 nc\tau\omega^2}$$

$$\omega_p = \sqrt{\frac{Ne^2}{m^* \varepsilon_{opt} \varepsilon_0}}$$

Wang, T; Radovanovic, P. V. *J. Phys. Chem. C* **2011**, *115*, 406–413

# Origin of Difference in Plasmonic Properties

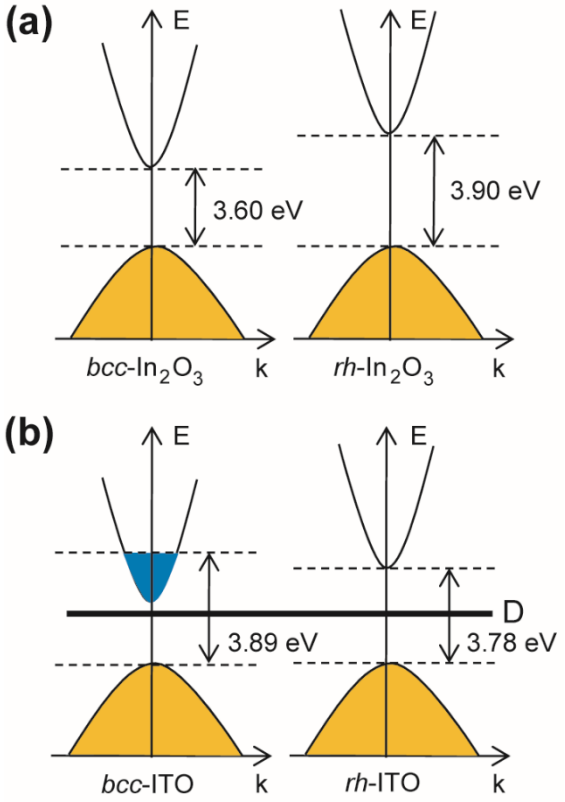


- **rh-$In_2O_3$ has larger band gap relative to bcc-$In_2O_3$**
- **This difference in electronic structure leads to larger donor activation energy in rh-ITO**
- **rh-$In_2O_3$ has low free carrier concentration in the conduction band**

Wang, T; Radovanovic, P. V. *J. Phys. Chem. C* **2011**, *115,* 406–413

# Expanding Plasmonic Properties in Mid-IR

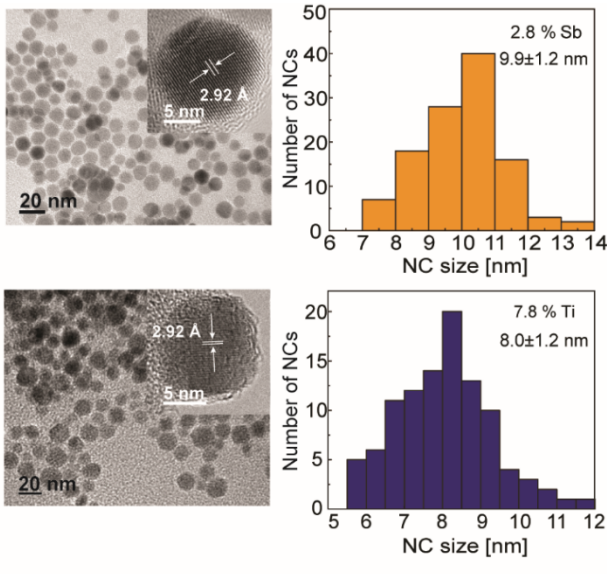


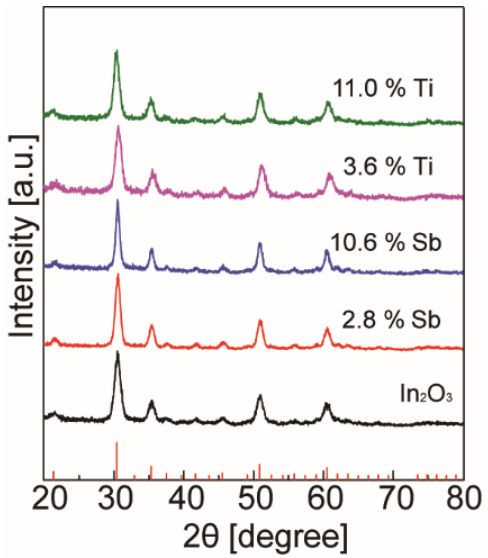


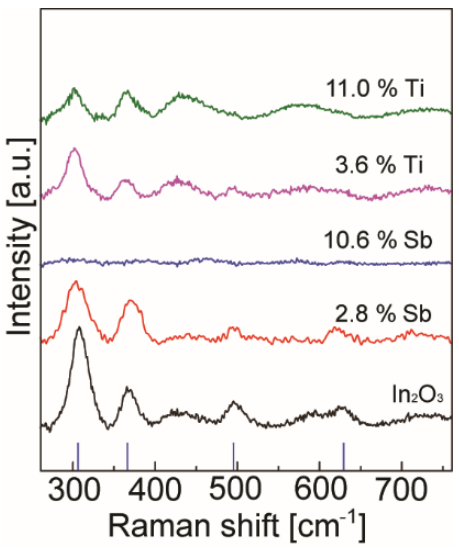


$Sb:In_2O_3$

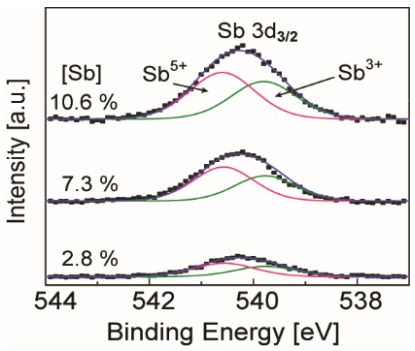


$Ti:In_2O_3$

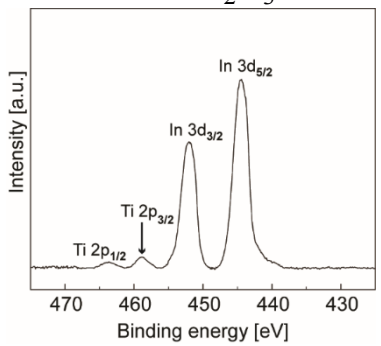


Fang, H.; Hegde, M.; Yin, P.; Radovanovic, P. V. *Chem. Mater.* **2017**, 29, 4970−4979.

# Tuning LSPR in Sb- and Ti-Doped $In_2O_3$ NCs

$Sb:In_2O_3$

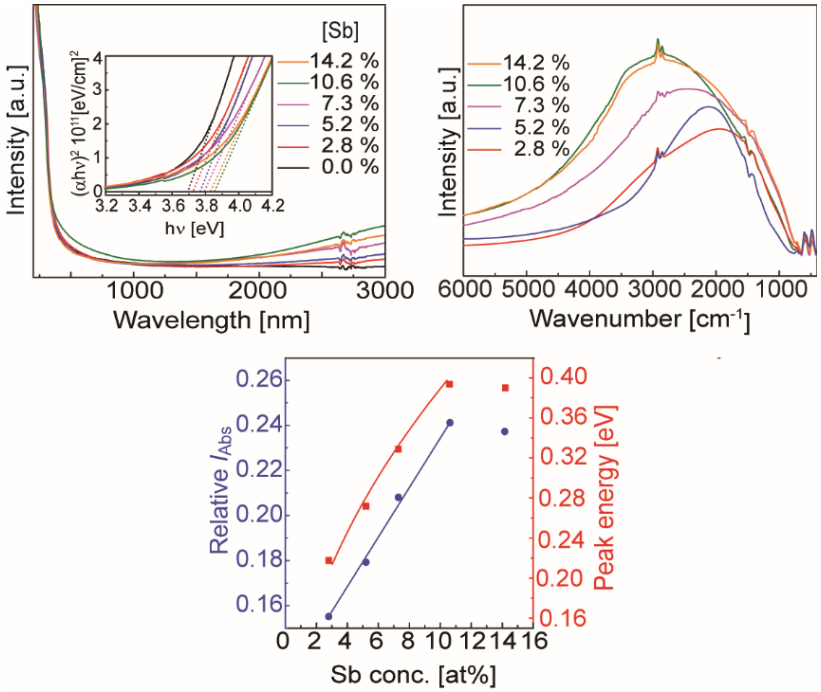


$Ti:In_2O_3$

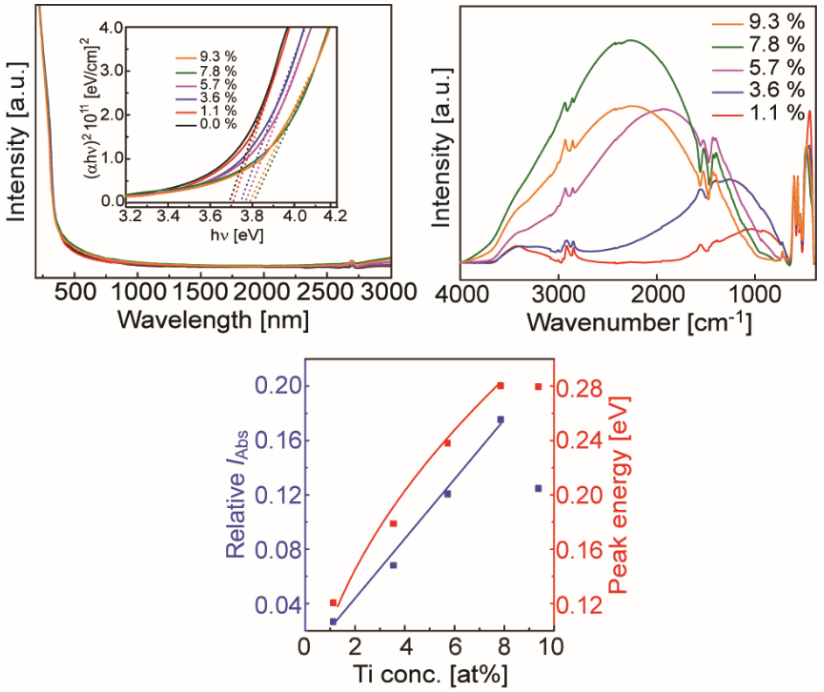


Fang, H.; Hegde, M.; Yin, P.; Radovanovic, P. V. *Chem. Mater.* **2017**, 29, 4970−4979

# Dopant-Dependence of Plasmonic Properties

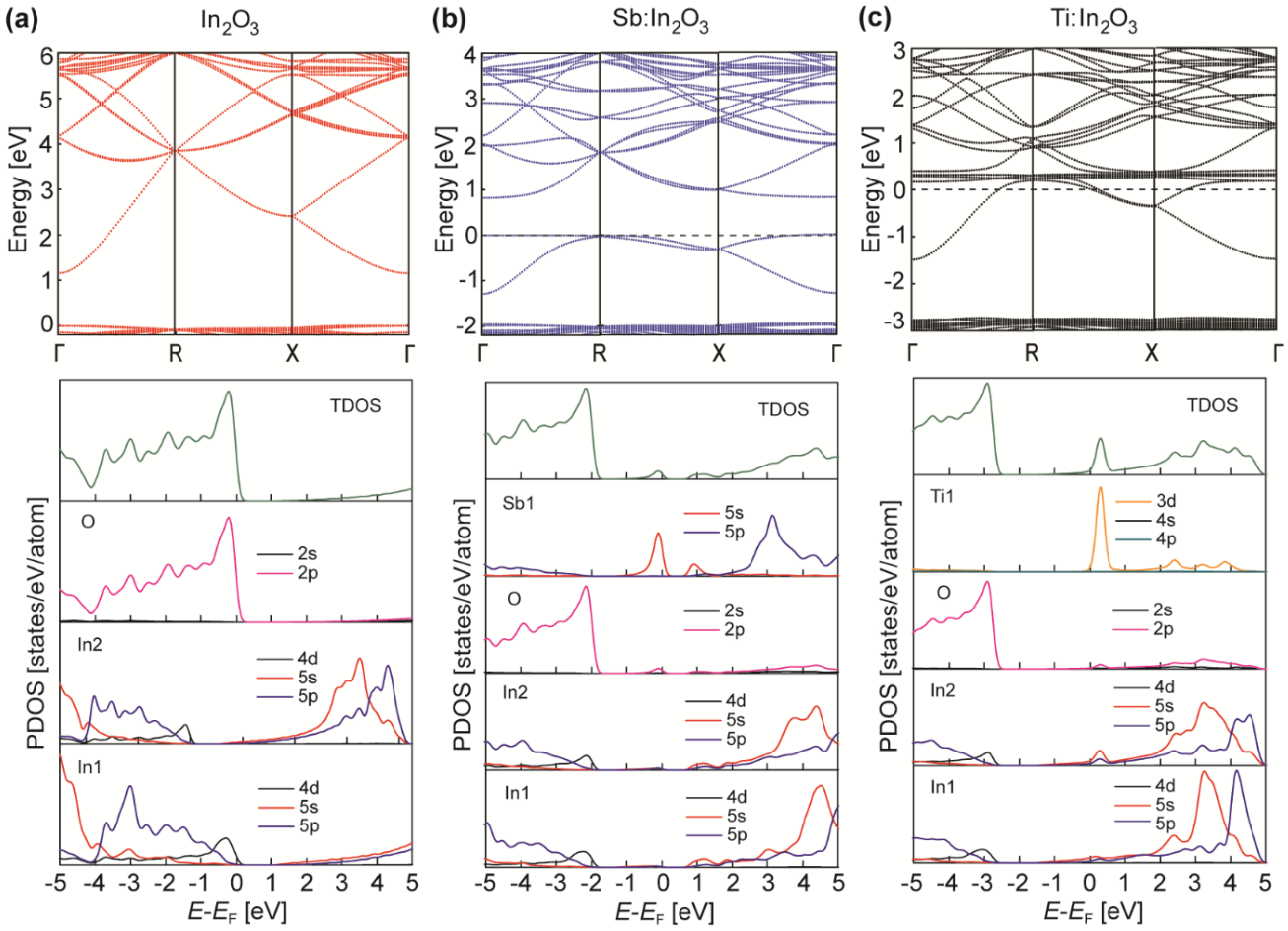

# s Trapping: Tuning LSPR in MIR

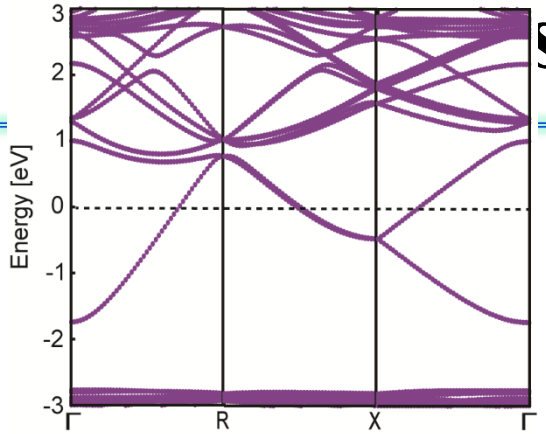


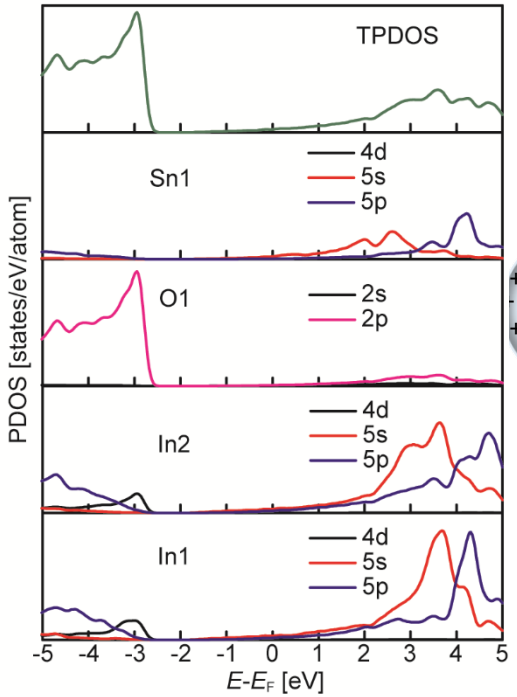


Ti:$In_2O_3$

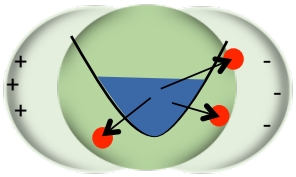

Sb:$In_2O_3$

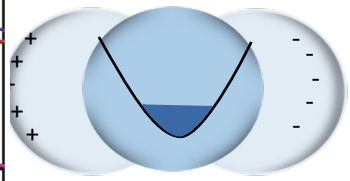

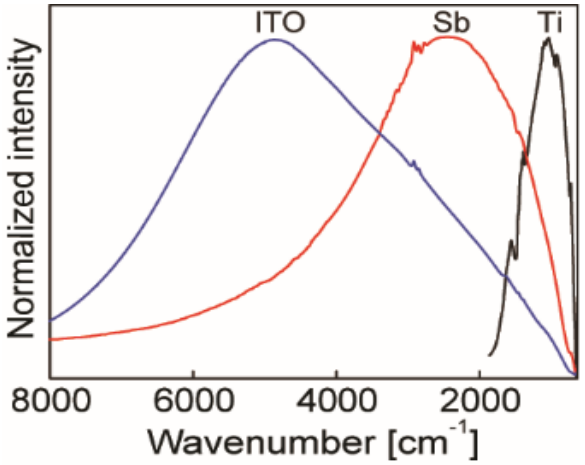


Fang, H.; Hegde, M.; Yin, P.; Radovanovic, P. V. *Chem. Mater.* **2017**, 29, 4970−4979

# Conclusions

- **Demonstrated in situ phase transformation of TMO NCs during colloidal synthesis.**

- **Critical size for stabilization of metastable rhombohedral $In_2O_3$ is ca. 5 nm. Phase transformation from rhombohedral to cubic $In_2O_3$ occurs by surface or interface nucleation, and the mechanism can be controlled by various synthesis parameters.**

- **SN and IN mechanisms have similar activation energies, which is consistent with the narrow phase transformation temperature range.**

- **Plasmonic properties of $In_2O_3$ NCs are strongly phase and dopant and electronic structure dependent, allowing for broad tunability of LSPR**

- **Possibility of expanding functionalities and rationally tailoring the properties of complex nanostructures by materials design using chemical principles.**

Radovanovic, P. V. "Defect-Induced Optical and Magnetic Properties of Colloidal Transparent Conducting Oxide Nanocrystals"; in *Functional Metal Oxides: New Science and Novel Applications*. Ogale, S. B.; Venkatesan, T. V.; Blamire, M. (Editors); Wiley-VCH: Weinheim, **2013**, *Chapter 5*, pp. 163-195.

# Acknowledgements:


## Group members:

**Current:**

- Manu Hegde
- Paul Stanish
- Vahid Ghodsi
- Natalie Sisombath
- Brian Fernandes
- Terry Yin
- Hanbing Fang
- Enas Hosawi
- Susi Jin
- Yunyan Wang
- Yi Tan
- Johnathan Altenbeck
- Shuoyuan Chan

**Past:**

**Postdocs: Josh Byers, Baran Yildirim, Arunasish Layek, Ian Hosein, Vladimir Blagojevic**

**Graduate students: Shokouh Farvid, Ting Wang, Melanie Chiu, Lisa Hutfluss, Vadim Chirmanov, Tahereh Saber, Ling Ju, Mutalifu Abulikemu, Neeshma Dave**

## Collaborators:

**Profs. Zoran Miskovic (University of Waterloo), Brahim Lounis (University of Bordeaux)**

**Funding:** NSERC CRSNG; Canada Research Chairs; Canada Foundation for Innovation / Fondation canadienne pour l'innovation; Ontario Centres of Excellence (Where Next Happens); C[4]; Ontario Ministry of Research & Innovation; Canadian Light Source / Centre canadien de rayonnement synchrotron; ACS PRF


University of Waterloo

Radovanovic Research Group

# Band Structure Calculation of ITO

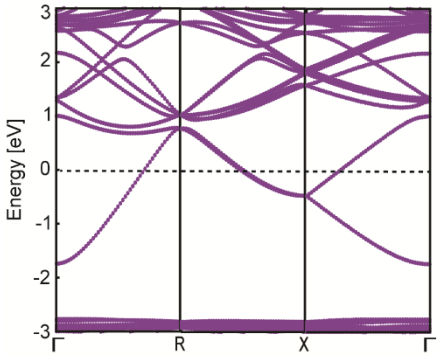


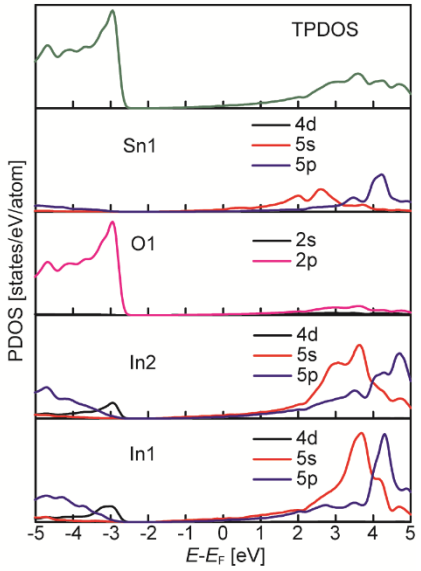


Fang, H.; Hegde, M.; Yin, P.; Radovanovic, P. V. *Chem. Mater.* **2017**, 29, 4970−4979

# Lighting Sources

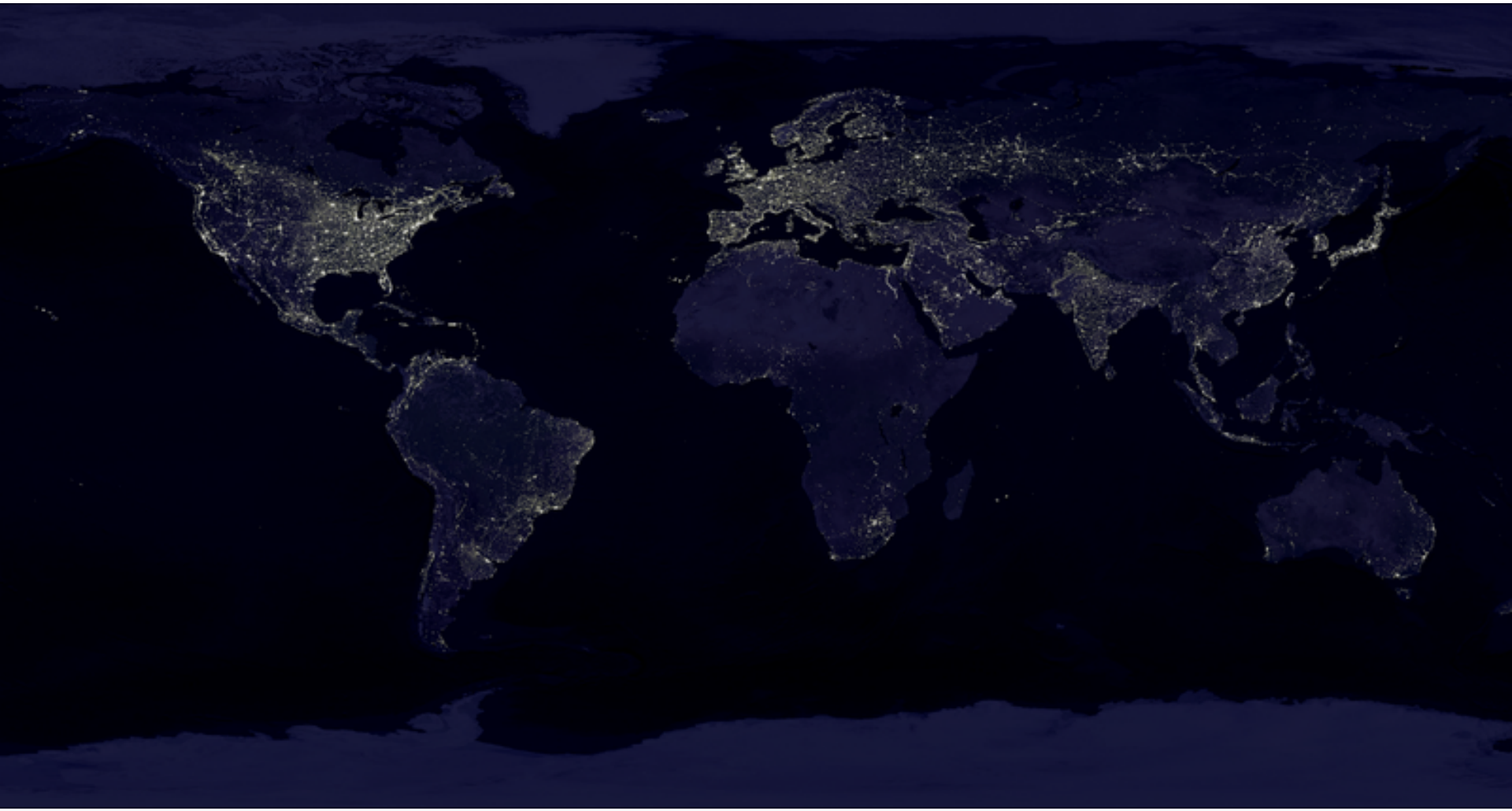

# Why is Lighting Source Significant?

• Lighting of homes, offices and public buildings accounts for more than 20 percent of the global electricity consumption, or ca. 3400 TWh

• 15-17% greater than nuclear or hydro power

• ca. 1900 $MtCO_2$ emission

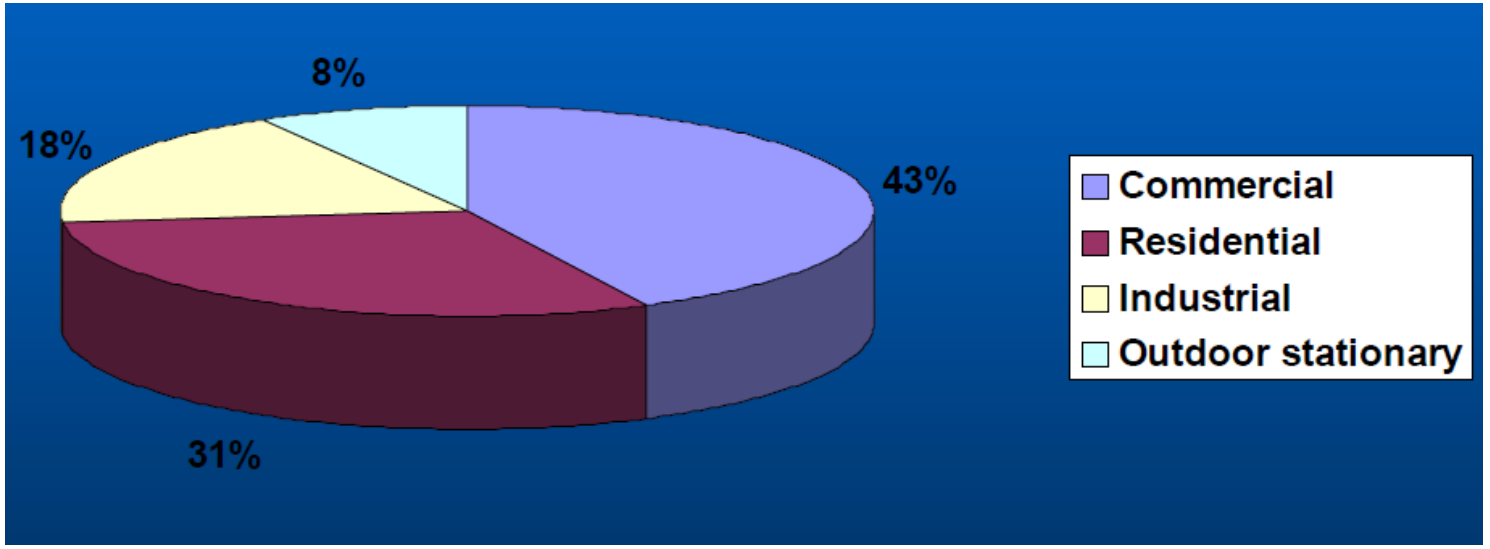


Hawken P. "*Natural Capitalism: Creating the Next Industrial Evolution*" Little, Brown & Co.: Boston, 1999.

# Average per Capita Electric Light Consumption

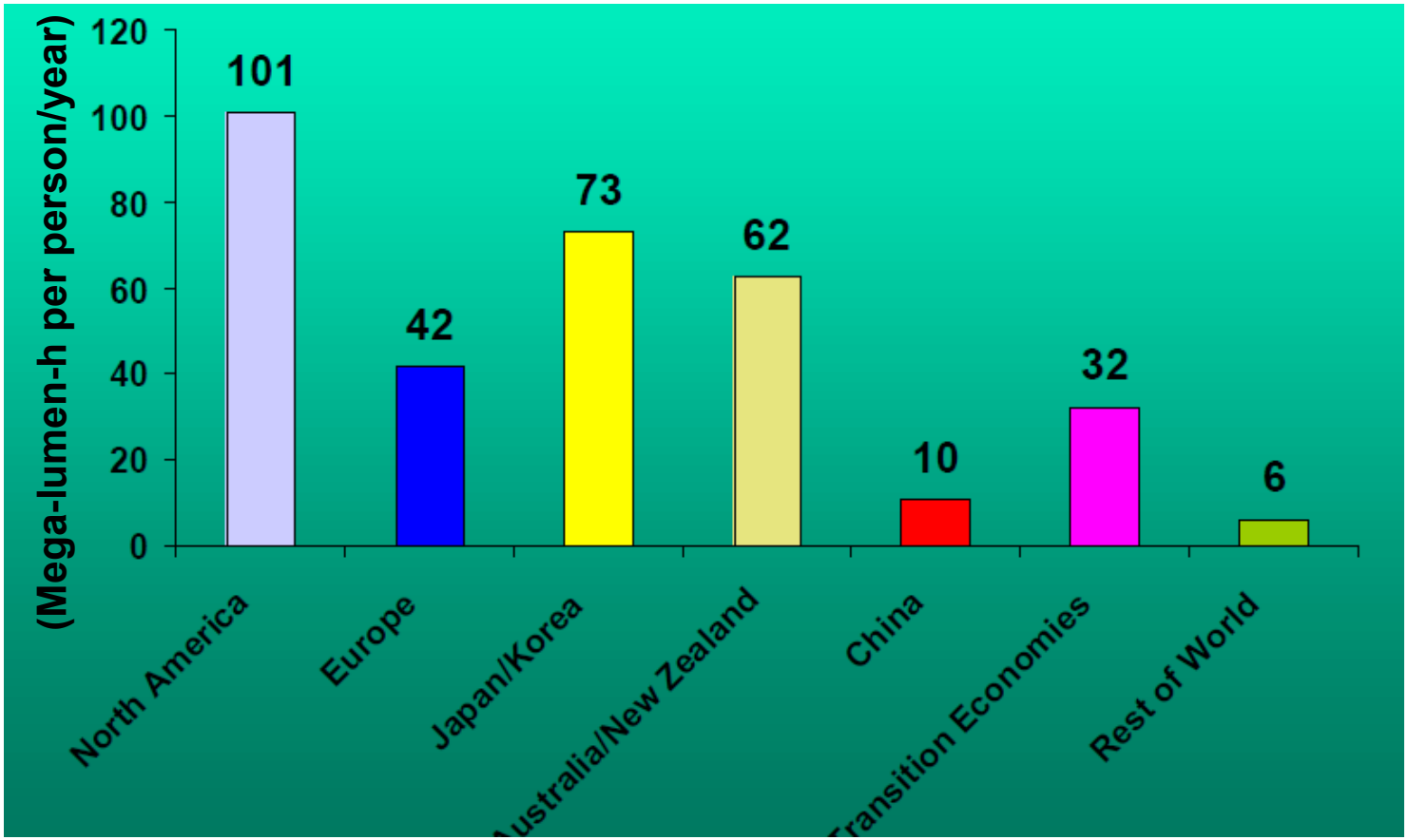


- A measure of human progress and development (expected to increase with economic development of emerging markets)

# Incandescent Light Bulbs

• Traditional incandescent light bulbs have only ca. 5% efficiency

• They are expected to be phased out worldwide in  the next 2 years, and replaced with more energy efficient devices.

• Ban on 100 and 75 lumens/Watt incandescent bulbs started in 2014; 60 and 40 lumens/Watt bulbs followed

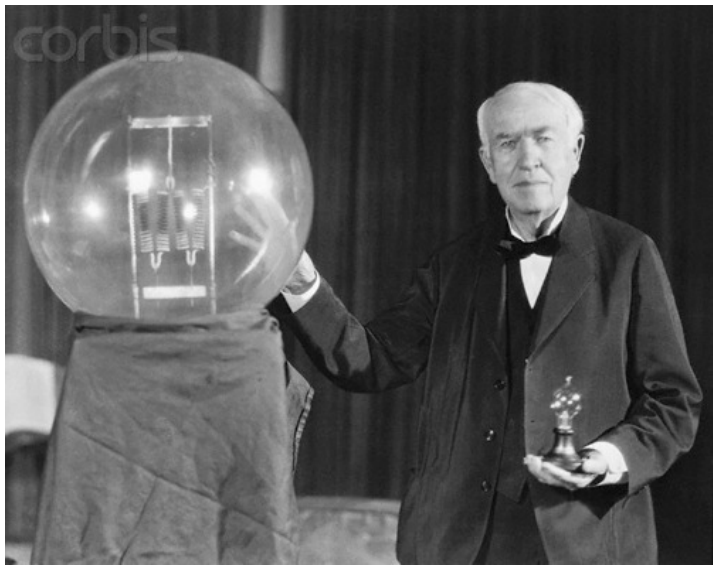


# Fluorescent and Induction Lamps

- It is based on electrical discharge or magnetic induction
- Both contain mercury; have bulky design; high CCT and low CRI.
- Induction lamp has the longest life of any light source 85,000-100,000 hours; efficient and no flickering; robust and durable-good for large area illumination; radio interference is a major issue; still expensive and under-commercialized

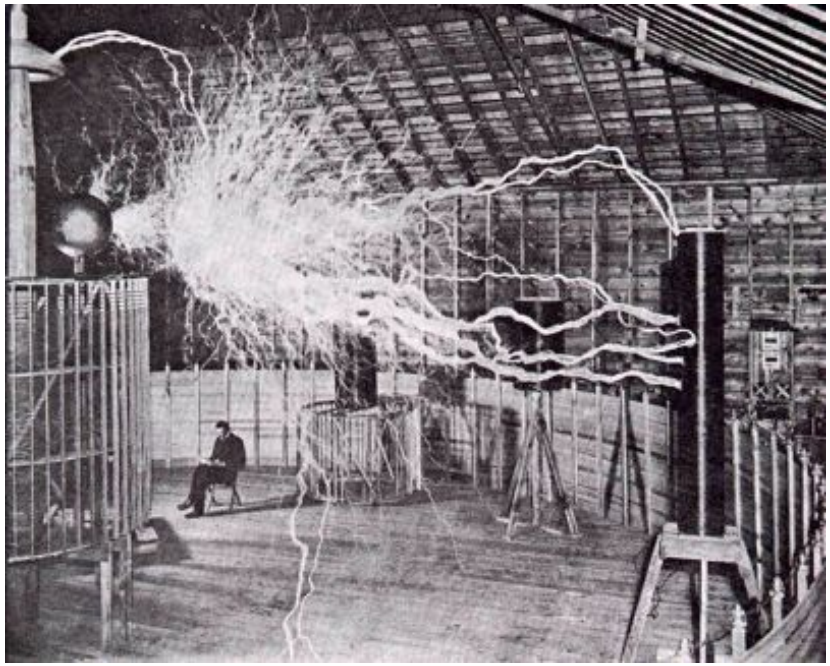

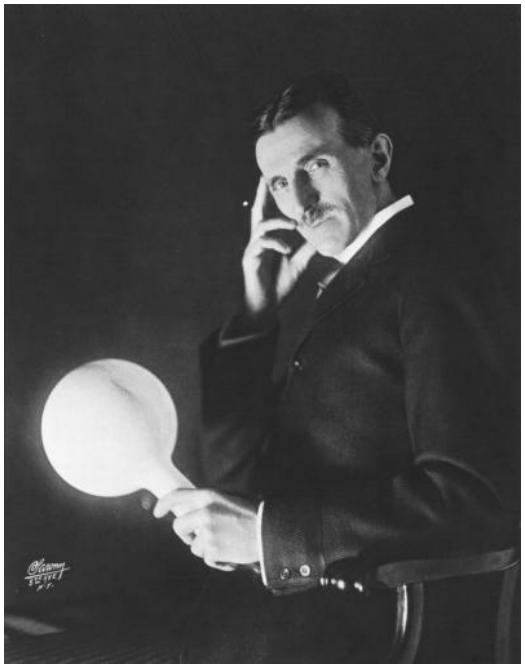

# Incandescent vs Induction Lamps

"***Surely, my system is more important than the incandescent lamp***, *which is but one of the known electric illuminating devices and admittedly not the best. Although greatly improved through chemical and metallurgical advances and skill of artisans it is still inefficient, and* ***the glaring filament emits hurtful rays responsible for millions of bald heads and spoiled eyes***. *In my opinion, it will soon be superseded by the electrodeless vacuum tube which I brought out thirty-eight years ago, a lamp much more economical and yielding a light of indescribable beauty and softness.*"

Nikola Tesla (1929)

# Light Emitting Diodes (LEDs)

Oleg V. Losev
(1903-1942)

CII. *Luminous Carborundum Detector and Detection Effect and Oscillations with Crystals.* *By* O. V. Lossev *.

[Plates XVII.–XX.]

Abstract.

In this paper are described further observations on the phenomenon of the luminescence produced at the contact of a carborundum detector in connexion with a view on luminescence as a consequence of the process in the contact which is very similar to cold electronic discharge.

Losev, O. V. *Phil. Mag.* **1928**, *6*, 1024-1044

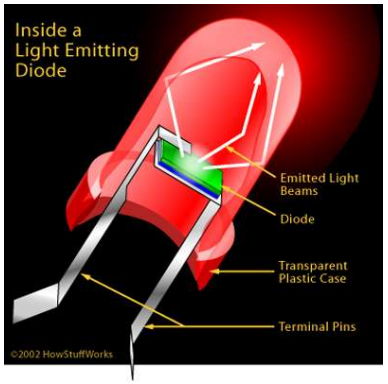


• LEDs have a number of advantages over conventional illumination sources: lower power consumption (up to 90 % less energy than traditional incandescent bulbs), extended lifetime (useful lifetime of up to 50,000 hours), smaller size, improved durability and reliability.

**So why are we not using LEDs more as a lighting source?**

# Current Design of White LEDs

• Combining LEDs with blue, green and red outputs in a final device to give an illusion of white light.

• Coating UV or blue LEDs (usually based on III-V semiconductors – GaN, GaInN or AlN) with phosphors emitting complementary colors

• Coating UV or blue LEDs with doped phosphors, such as Ce:YAG (a yellow emitter) giving off quasi-white light upon illumination.

• Organic LEDs (OLEDs): generally cheap and easily processable, but may involve complex synthetic procedure, and are less efficient and less stable than inorganic-based LEDs.

**•Barriers to LED adoption: design complexity, cost and quality of white light**

# Size-Determined Stabilization of γ-$Ga_2O_3$

- **Gallium oxide is stabilized in metastable phase below critical size (ca. 6 nm)**

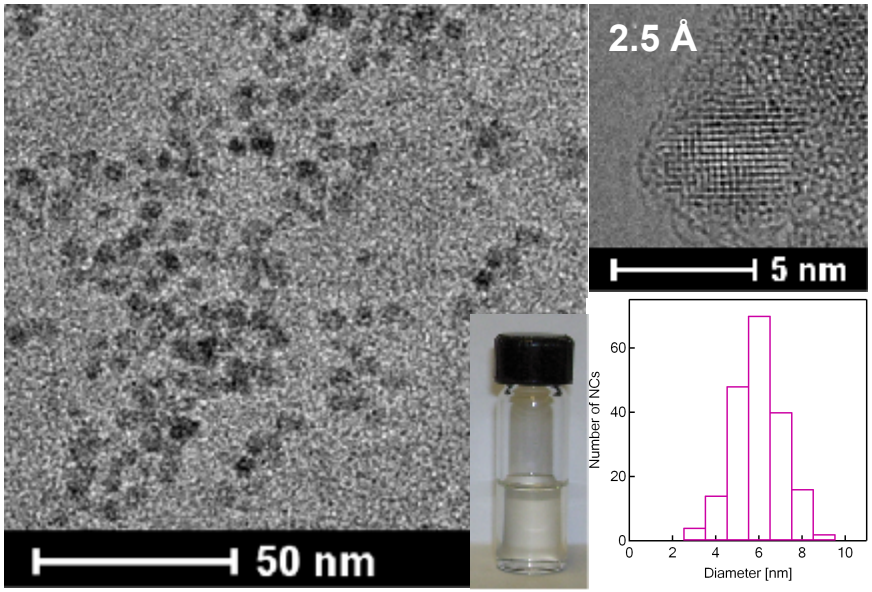


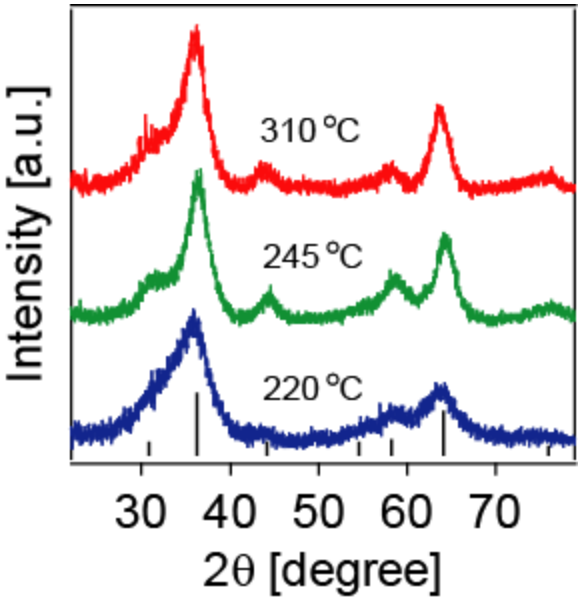


Wang, T.; Farvid, S. S.; Abulikemu, M.; Radovanovic, P. V., *J. Am. Chem. Soc.* **2010**, 132, 9250

# Phase Dependence of PL Properties: $Ga_2O_3$

- Different native defect electronic structure leads to phase-dependence of PL properties

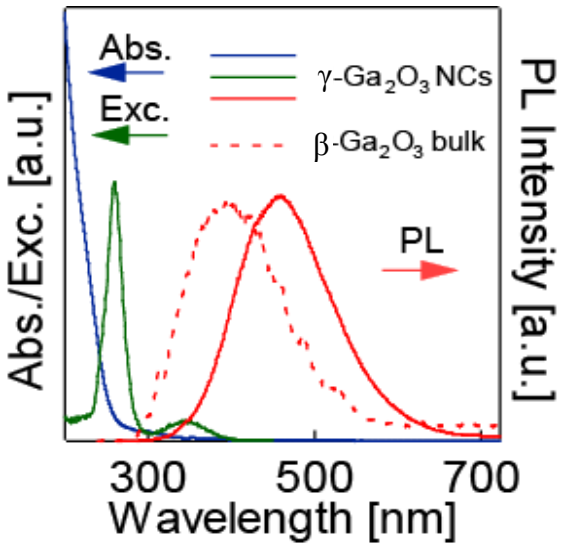


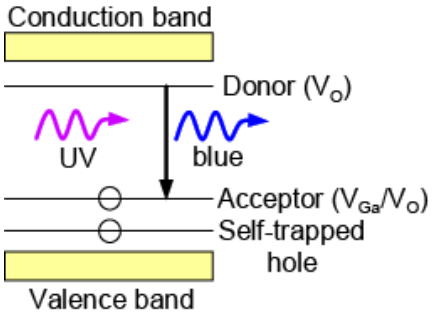


$$O_O^x \rightarrow V_O^x + \frac{1}{2}O_2 \rightarrow V_O^{\bullet} + \frac{1}{2}O_2 + e^-$$

$$\left(V_O, V_{Ga}\right)' + V_O^{\bullet} + h\nu \leftrightarrow \left(V_O, V_{Ga}\right)^x + V_O^x$$

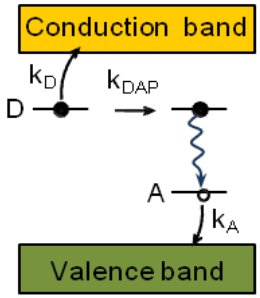


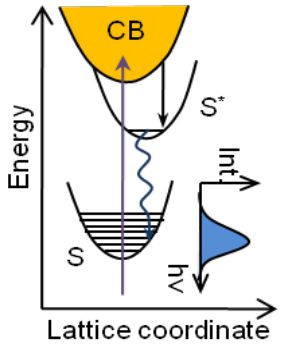


- PL broadening originates from phonon coupling and a range of defect separations

Wang, T.; Farvid, S. S.; Abulikemu, M.; Radovanovic, P. V., *J. Am. Chem. Soc.* **2010**, 132, 9250

# Size Dependence of PL Properties

- Size tunability of the PL associated with Coulomb interactions of charged donors and acceptors

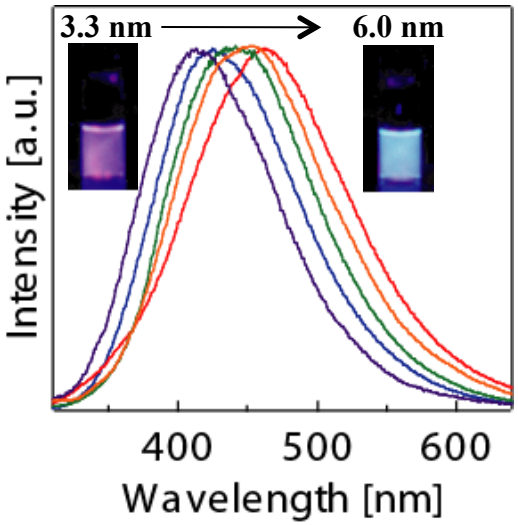


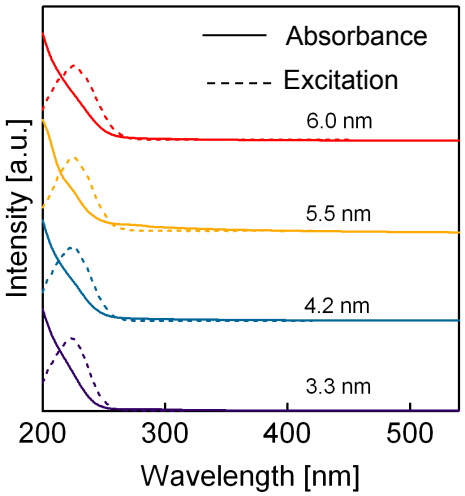


$$I(T) = \frac{I_0}{1 + A\exp(-\Delta E/kT)}$$

| NC size [nm] | $I_0$ [a.u.] | A [a.u.] | ΔE [mev] |
|---|---|---|---|
| 6.0 nm | 32.92 | 1443.8 | 204.94 |
| 4.2 nm | 35.66 | 3457.8 | 221.80 |
| 3.3 nm | 38.95 | 8120.4 | 238.41 |

$$E = E_g - (E_D + E_A) + E_C \pm nE_{phonon}$$

- Negligible quantum confinement effect

$$E_C = \frac{e^2}{4\pi\varepsilon r}$$ Coulomb interaction term

*J. Am. Chem. Soc.* **2010**, 132, 9250

*J. Phys. Chem. C* **2011** *115*, 18473

# Donor-Acceptor Pair Modeling

The recombination rate,

$$W(r)=W_{max}\ exp(-2r/R_d)$$

If Q is the probability that an electron on the donor,

$$dQ/dt=-Q\sum_j W(r_j),\ Q(t)=exp(-\sum_j W(r_j)t)$$

$$\langle Q(t)\rangle=1/V^N \int_V \int \ldots \int exp\{-\sum_j W(r_j)\,t\}\, d^3 r_1\, d^3 r_2 \ldots d^3 r_N$$

$$\langle Q(t)\rangle=[1+1/N\ n\int_0^\infty \{exp[-W(r)t]-1\}d^3 r\,]^N$$

As $N\to\infty$, $V\to\infty$, but $N/V=n$ (finite),

$$\langle Q(t)\rangle=exp[4\pi n\int_0^\infty \{exp[-W(r)t]-1\}r^2\,dr\,]$$

Intensity of the emitted light, $I(t)=-d\langle Q(t)\rangle/dt$

Thomas, D.G.; Hopfield, J. J.; Augustyniak, W. M. *Phys. Rev.* **1965**, *140*, A202-A220

# Theoretical Simulations (3D Model)

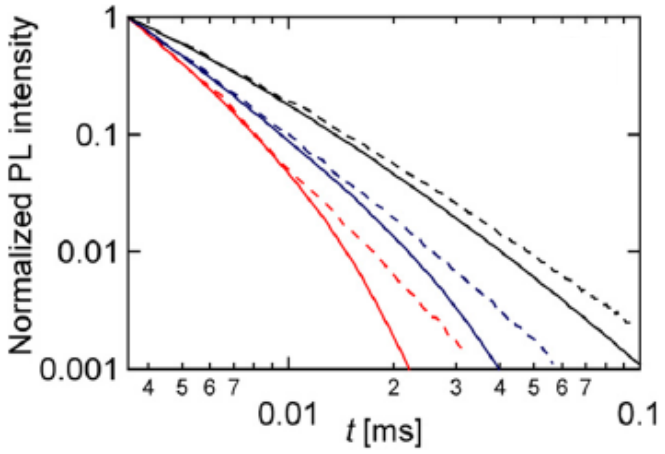


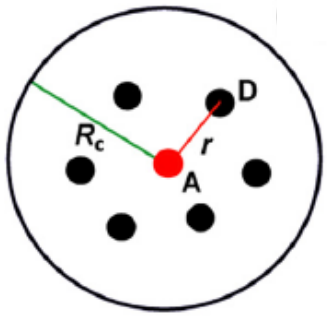


$R_d$=0.9 nm, $W_{max}=10^7$ sec$^{-1}$

$R_c$ = 1.6 nm
$R_c$ = 2.1 nm
$R_c$ = 3.0 nm

$$\langle Q(t)\rangle = exp[4\pi n \int_0^{R_c} \{exp[-W(r)t]-1\} r^2 dr]$$

$$x=r/R_c \ , N_D = 4\pi/3 \ R_c^3 \ n, \tau = t \ W_{max}$$

$$\gg 1, \ \rho = R_c/R_d > 1$$

(1)

$$I(\tau) = 3 \ W_{max} N_D \ J_2 \ exp[3 \ N_D \ (e^{-\tau} e^{-2\rho} - 1 - 2\rho\tau J_3)]; \ J_i = \int_0^{\infty} x^i e^{-2\rho x} e^{-\tau e^{-2\rho x}} dx$$

Hegde, M., Wang, T., Miskovic, Z. L., Radovanovic, P. V. *Appl. Phys. Lett.*, **2012**, *100*, 141903.

# Theoretical Simulations (2D Model)

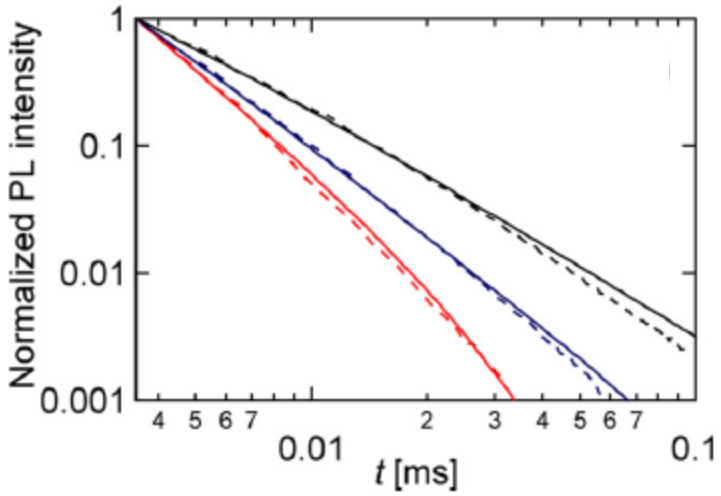


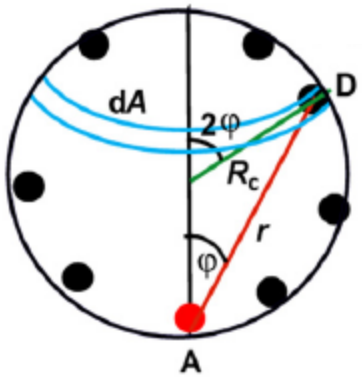


$R_d$=1.1 nm, $W_{max}=10^7$ sec$^{-1}$

$R_c$ = 1.65 nm
$R_c$ = 2.1 nm
$R_c$ = 3.0 nm

$$\langle Q(t)\rangle = exp[4\pi Rc\downarrow\uparrow 2\ n\int 0\uparrow\pi/2\ \blacksquare \sin(2\varphi)\ \{\exp[-t\,W\,(2\,R\downarrow c\cos\varphi)]-1\}d\varphi\ ]$$

$$x=\cos\varphi\,,\ r=2R\downarrow c\cos\varphi,\ N\downarrow D=4\pi R\downarrow c\uparrow 2\ n,\ \tau=t\ W\downarrow max\gg 1,$$

$$I(\tau)=2\ WmaxN\downarrow D\ \ J\downarrow 1\ exp[N\downarrow D\ (e\uparrow-\tau\ e\uparrow-4\rho\ -1-4\ \rho\ \tau\ J\downarrow 2\ )]\ ;\ J\downarrow i=\int 0\uparrow\blacksquare\ x\uparrow i\ e\uparrow-4\ \rho x\ e\uparrow-\tau\ e\uparrow-4\ \rho x\ dx$$

- Subtle result: decreased NC size leads to an increase in donor binding energy

# Tunable White Light Generation

• $Ga_2O_3$ nanocrystal DAP blue emission is sufficiently broad and tunable in the exactly right region to require only addition of a narrow spectral density in orange-red

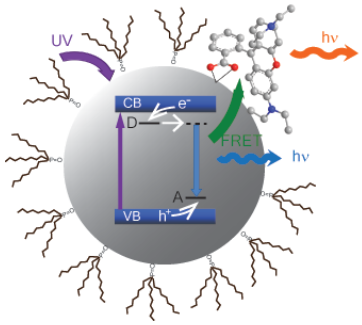


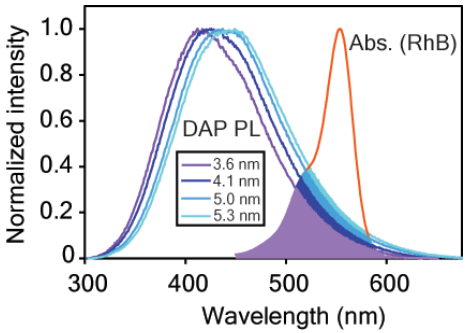


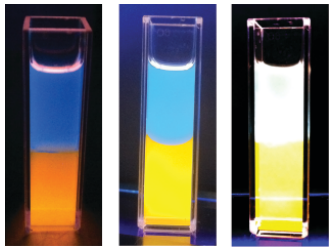

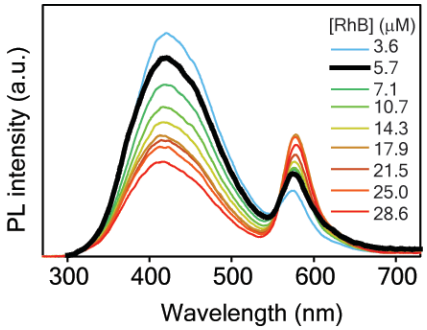


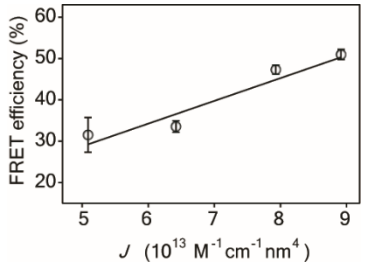


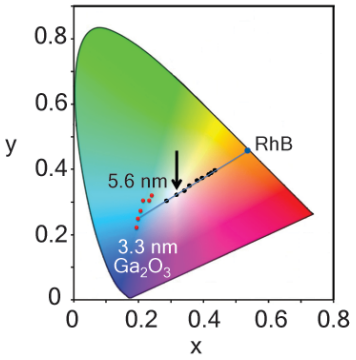


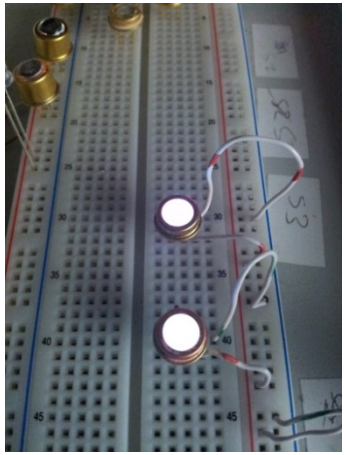


Wang, T.; Radovanovic, P. V. *U.S. Patent Appln.* **2015**, No. 20150108406

Wang, T.; Chirmanov, V.; Chiu, M. H. W.; Radovanovic, P. V. *J. Am. Chem. Soc.* **2013**, *135*,14520

Chirmanov, V.; Stanish, P.; Layek, A.; Radovanovic, P. V. *J. Phys. Chem. C* **2015**, *119*, 5687-5696

# Quasi Single Chromophore

- RhB PL decays on ns timescale upon direct excitation; lifetime changes insignificantly when bound to $Ga_2O_3$
- RhB adopts $Ga_2O_3$ decay timescale after binding (when excited into $Ga_2O_3$ band gap)

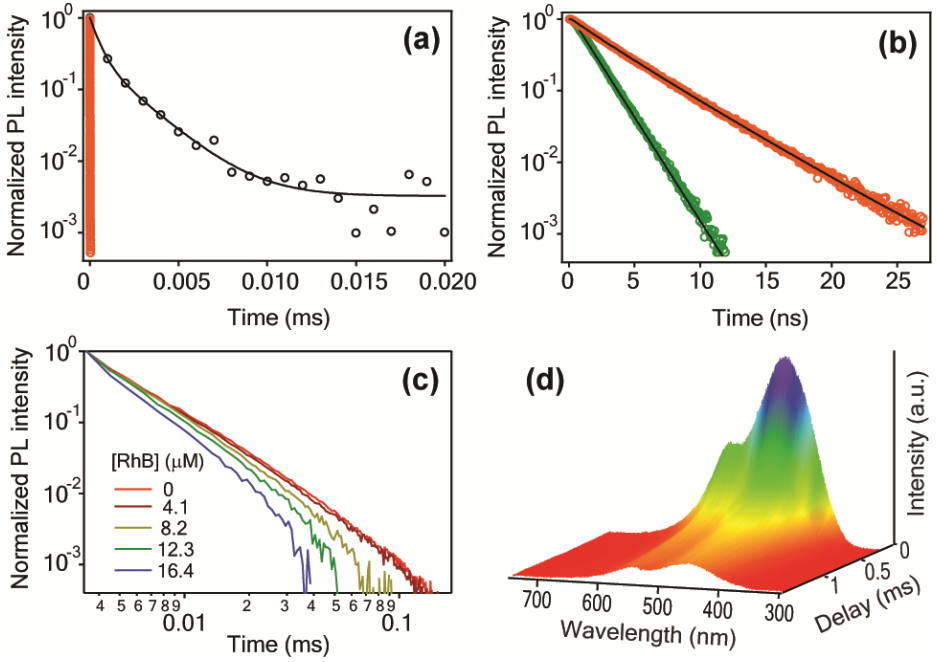

# Generality: ZnO NC-Based NanoLite

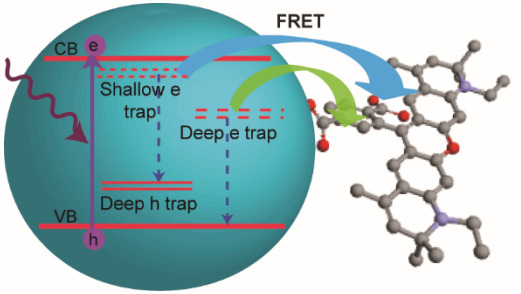


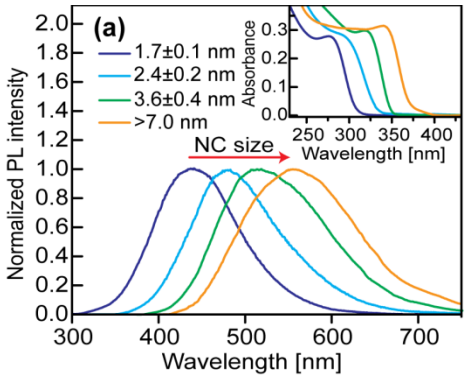


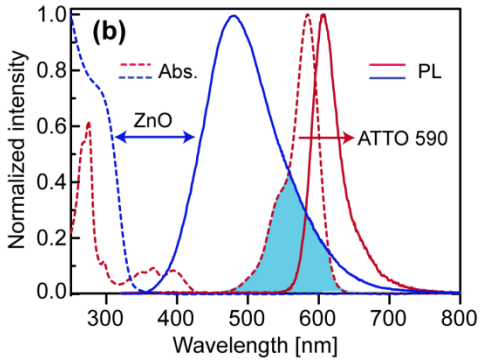


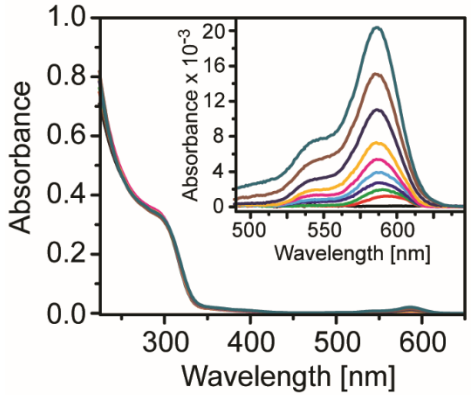


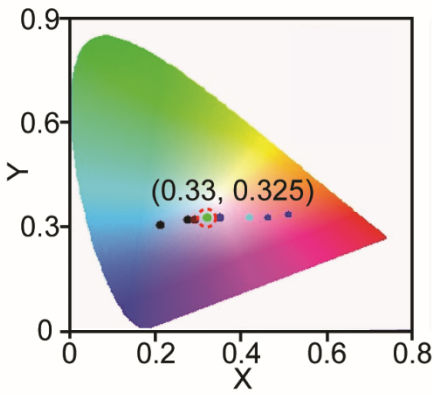


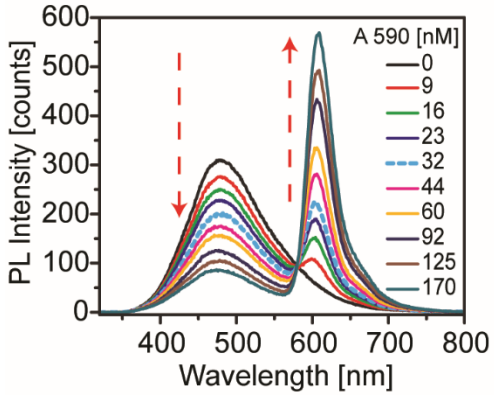


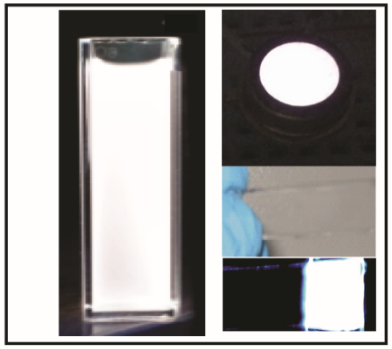

*US Patent Appl.* **2016**, No. 20160102842
Layek et al. *Chem. Mater.*, **2015**, *27*, 1021-1030

# Optimization and Stability

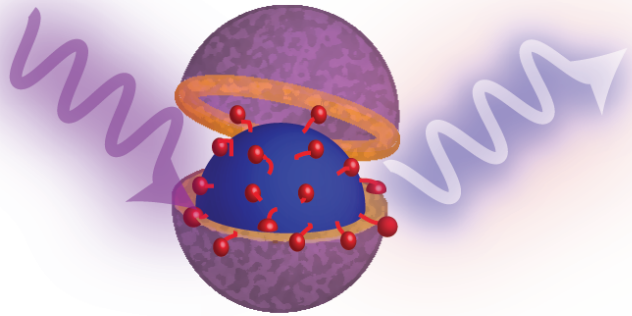

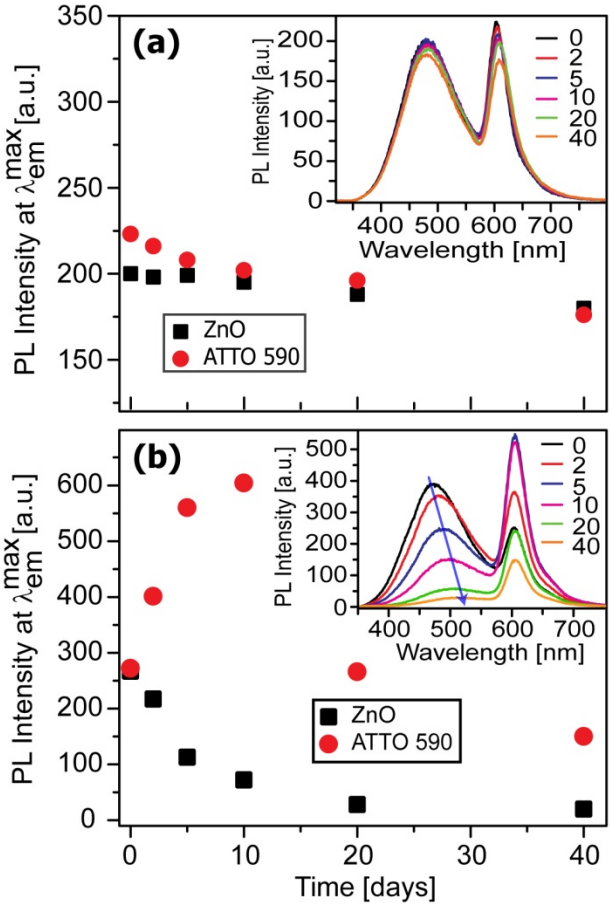


silane layer

non-protected

Layek A.; Stanish, P. C.; Chirmanov, V.; Radovanovic, P. V. *Chem. Mater.*, **2015**, *27*, 1021-1030
*US Patent Appl.* **2016**, No. 20160102842

# Broad UV Range Conversion

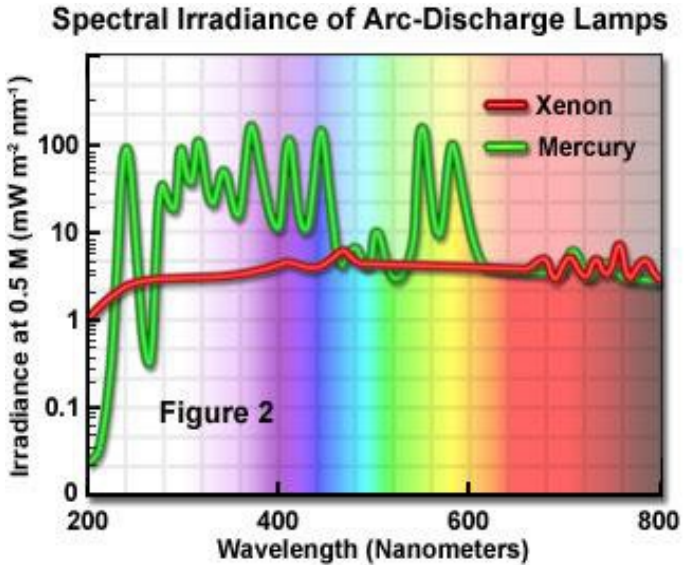


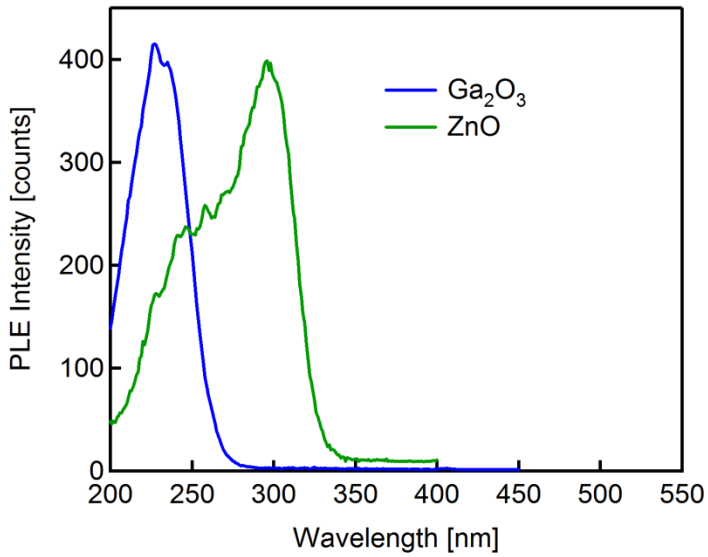


- Chromaticity, homogeneity and light characteristics independent of composition
- Different excitation for the same emission: increasing efficiency

# All-Inorganic White Light Emitting Phosphors

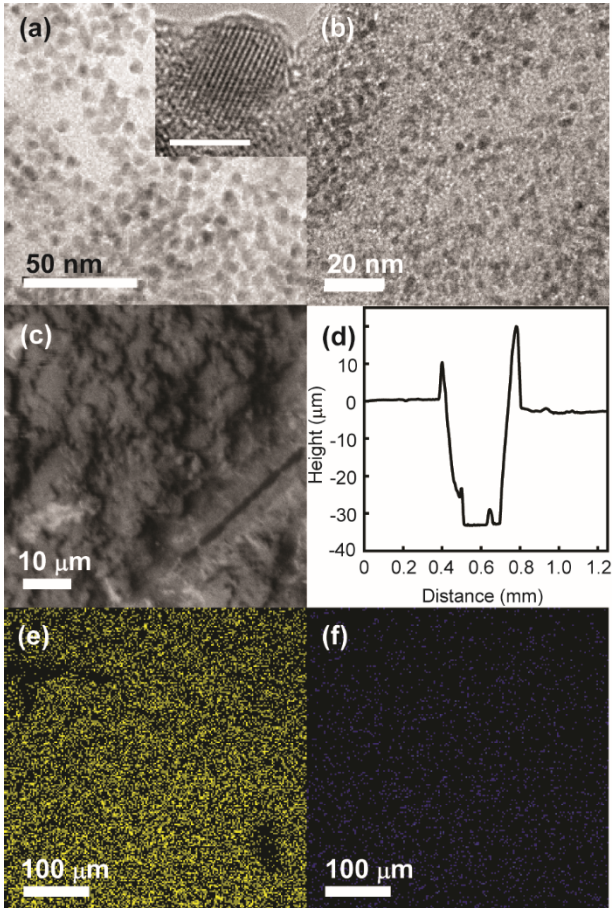


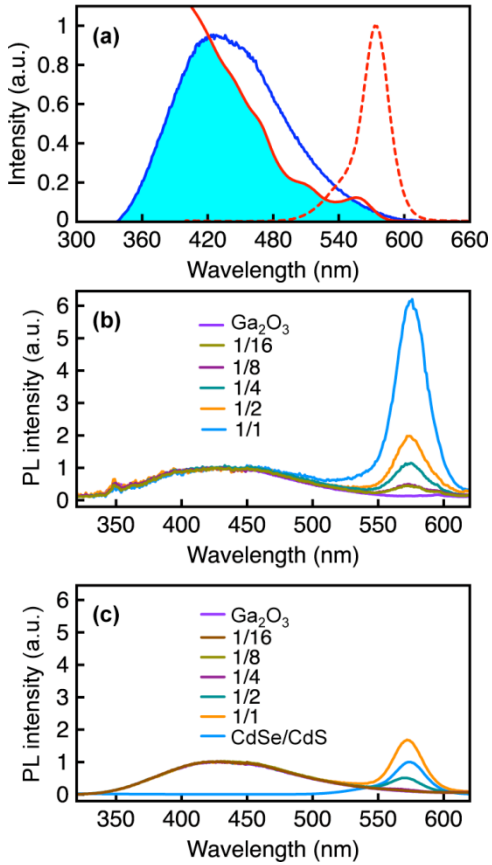


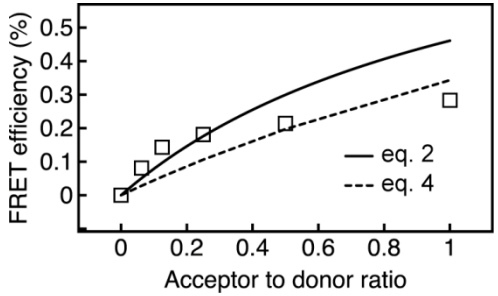


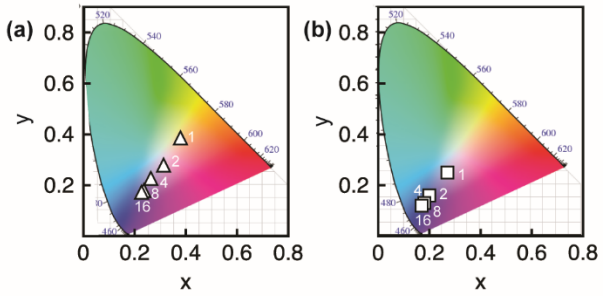


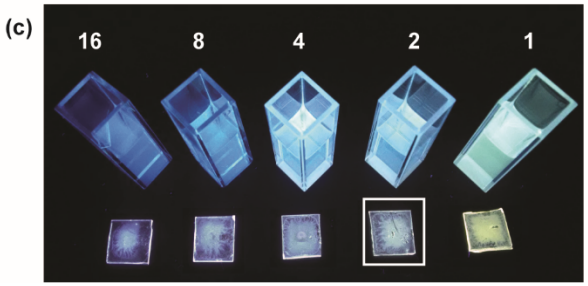


Stanish, P. C.; Radovanovic, P. V. *J. Phys. Chem. C*, **2016**, in press

# Conclusions

- **Demonstrated in situ phase transformation of TMO NCs during colloidal synthesis.**

- **Critical size for stabilization of metastable rhombohedral $In_2O_3$ is ca. 5 nm. Phase transformation from rhombohedral to cubic $In_2O_3$ occurs by surface or interface nucleation, and the mechanism can be controlled by various synthesis parameters.**

- **SN and IN mechanisms have similar activation energies, which is consistent with the narrow phase transformation temperature range.**

- **Phase transformation, nanocrystal size and reaction conditions all lead to variation in the defect electronic structure, which can be used to control optical properties (tunable white light generation).**

- **Possibility of expanding functionalities and rationally tailoring the properties of complex nanostructures by materials design using chemical principles.**

Radovanovic, P. V. "Defect-Induced Optical and Magnetic Properties of Colloidal Transparent Conducting Oxide Nanocrystals"; in *Functional Metal Oxides: New Science and Novel Applications*. Ogale, S. B.; Venkatesan, T. V.; Blamire, M. (Editors); Wiley-VCH: Weinheim, **2013**, *Chapter 5*, pp. 163-195.

# Acknowledgements:


## Group members:

**Current:**

- Manu Hegde
- Paul Stanish
- Vahid Ghodsi
- Natalie Sisombath
- Brian Fernandes
- Terry Yin
- Hanbing Fang
- Enas Hosawi
- Susi Jin
- Yunyan Wang
- Yi Tan
- Johnathan Altenbeck
- Shuoyuan Chan

**Past:**

**Postdocs: Josh Byers, Baran Yildirim, Arunasish Layek, Ian Hosein, Vladimir Blagojevic**

**Graduate students: Shokouh Farvid, Ting Wang, Melanie Chiu, Lisa Hutfluss, Vadim Chirmanov, Tahereh Saber, Ling Ju, Mutalifu Abulikemu, Neeshma Dave**

## Collaborators:

**Profs. Zoran Miskovic (University of Waterloo), Brahim Lounis (University of Bordeaux)**

**Funding:** NSERC CRSNG; Canada Research Chairs; Canada Foundation for Innovation / Fondation canadienne pour l'innovation; Ontario Centres of Excellence (Where Next Happens); C[4]; Ontario Ministry of Research & Innovation; Canadian Light Source / Centre canadien de rayonnement synchrotron; ACS PRF


University of Waterloo

Radovanovic Research Group

# Plasmonic Nanocrystals

- The localized surface plasmon resonance (LSPR) is the result of the collective oscillation of conduction electrons in the particle upon interaction with light.

- The resonant conditions of the plasmon are sensitive to the surrounding medium – suitable applications as sensors, chemical probes, light concentrators in solar cells, surface-enhanced Raman spectroscopy (SERS)

- Gold and silver nanocrystals are most commonly used nanostructured plasmonic materials – easy to synthesize, relatively inert to oxidation and other reactions, have high carrier concentrations

- Issues with metal nanoparticles: high optical losses (due to electronic transitions), cost, large real component of the dielectric constant.

- Dielectric nanoparticles can be larger (easier to synthesize/fabricate)

# Effect of Dopants on the Host Structure

## XRD of ITO NCs

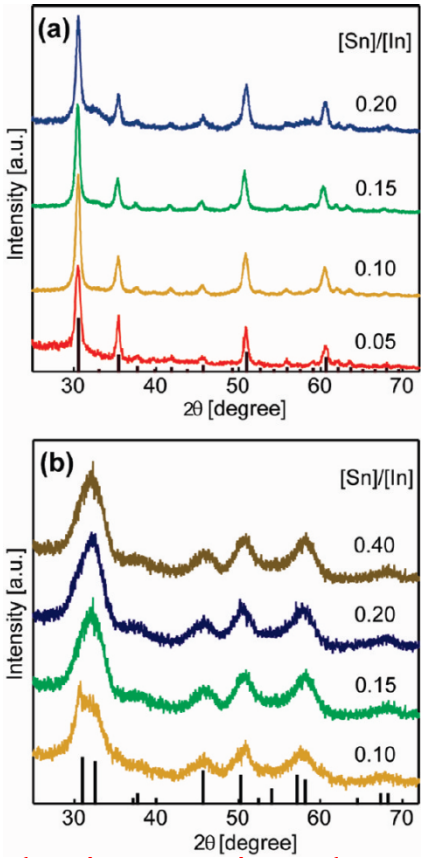


The increasing dopant precursor conc. leads to a decrease in NC size

## Raman spectrum of bcc-ITO

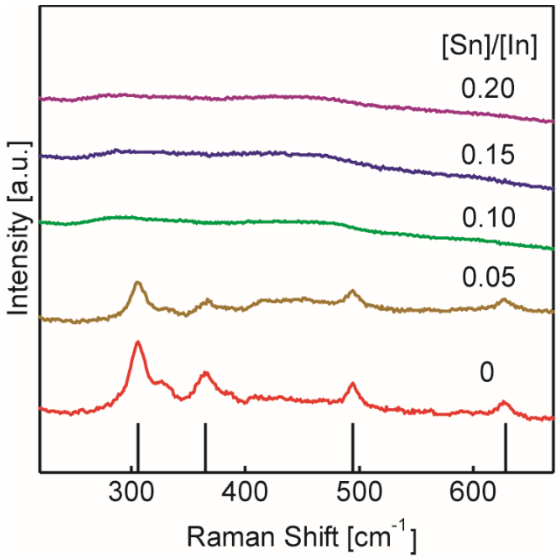


Decrease in phonon correlation lengths due to local crystal lattice disorder.

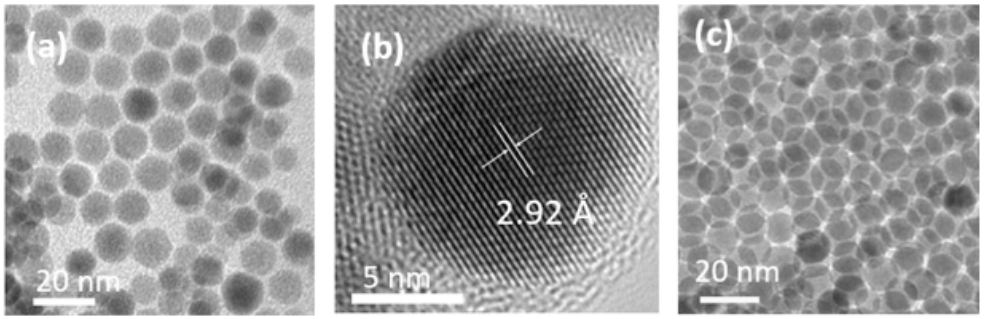

# NC Electronic Structure

## XPS spectroscopy of ITO NCs

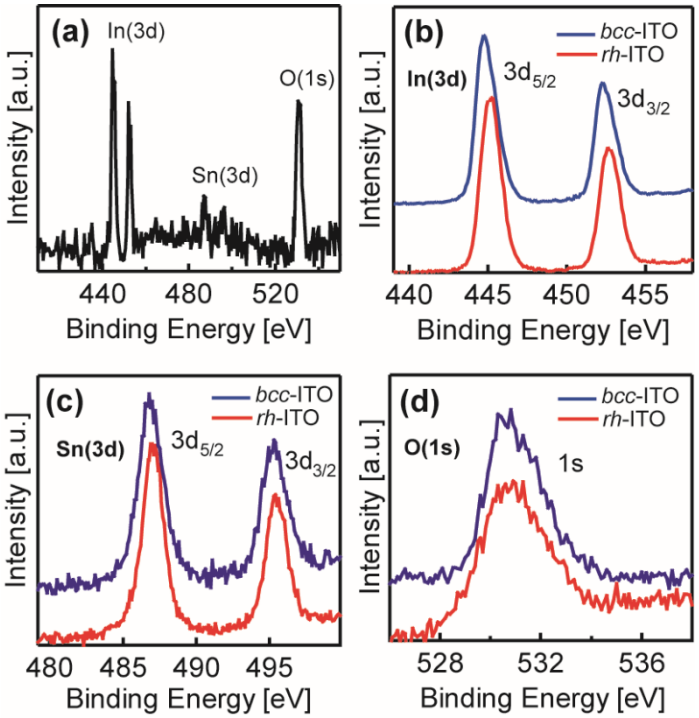


| starting $Sn^{4+}$ concentration ([Sn]/[In]) | $Sn^{4+}$ doping concentration in ITO NCs (at%) | |
|---|---|---|
| | bcc-ITO | rh-ITO |
| 0 | 0 | — |
| 0.05 | 4.5 | — |
| 0.10 | 8.6 | 9.0 |
| 0.15 | 12.3 | 13.8 |
| 0.20 | 18.5 | 17.4 |
| 0.40 | — | 32.7 |

- $Sn^{4+}$ occupies mostly b-site in bcc-ITO (substitutional doping)

Wang, T; Radovanovic, P. V. *J. Phys. Chem. C* **2011**, *115*, 406–413

# Plasmonic Properties of Colloidal ITO NCs

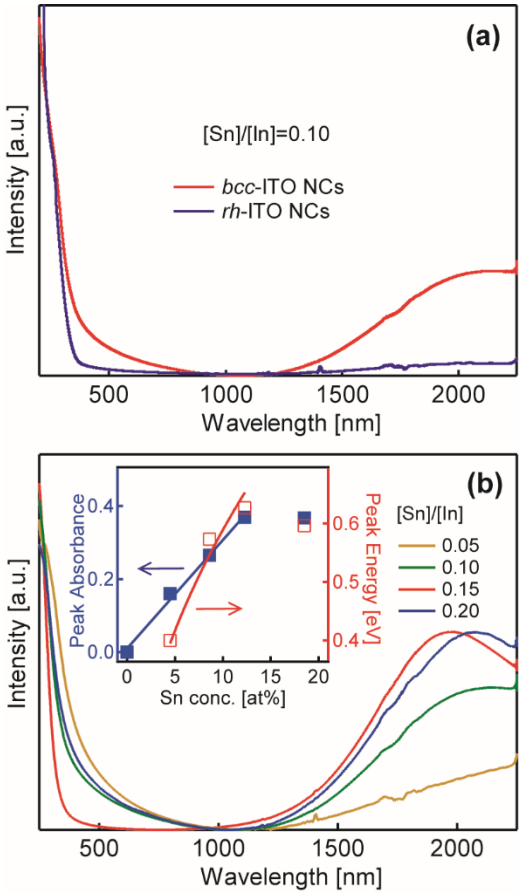


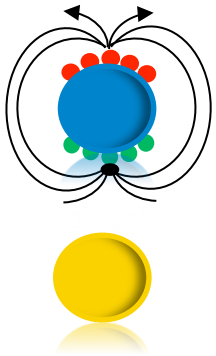

bcc-ITO

rh-ITO

## Drude-Lorentz Model

$$\alpha_{free-electrons} = \frac{Ne^2}{m^* \varepsilon_0 nc\tau\omega^2}$$

$$\omega_p = \sqrt{\frac{Ne^2}{m^* \varepsilon_{opt} \varepsilon_0}}$$

- Using the parameters for bulk bcc-$In_2O_3$ ($m^*$=0.3$m_0$, $\varepsilon_{opt}$=4.0) the maximum concentration of free electrons in bcc-ITO NCs is estimated to be ca. $3.3 \times 10^{20}$ $cm^{-3}$

# Origin of Difference in Plasmonic Properties

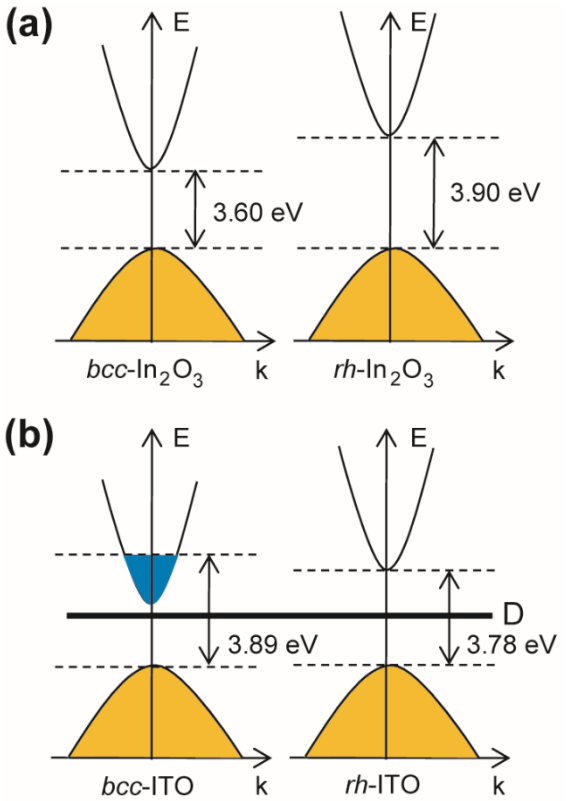


- **rh-$In_2O_3$ has larger band gap relative to bcc-$In_2O_3$**
- **This difference in electronic structure leads to larger donor activation energy in rh-ITO**
- **rh-$In_2O_3$ has low free carrier concentration in the conduction band**

# Plasmon Absorption Spectra of AIO NCs

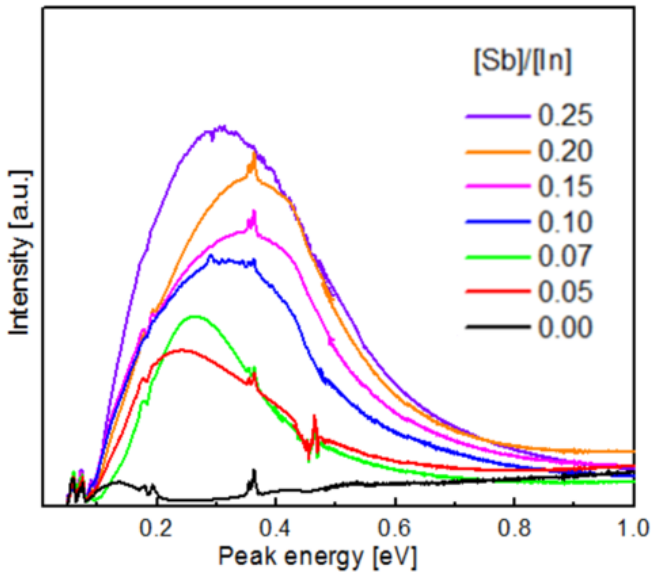


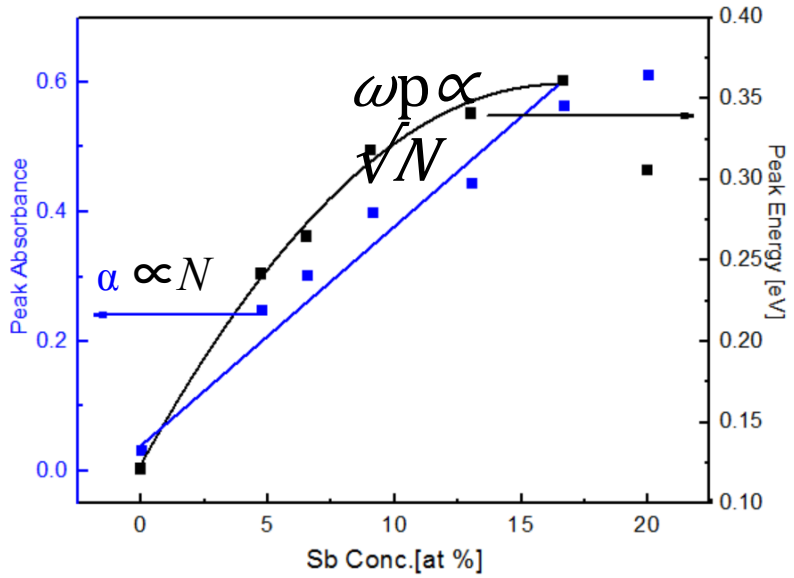


- **Plasmonic transitions observed in AIO NCs**
- **Resonance maxima shifted to lower energies relative to ITO NCs (mid-IR)**
- **$Sb^{3+}$ oxidized to $Sb^{5+}$**
- **Drude model behavior is also observed in AIO NCs**
- **$N=2.6 \times 10^{18}$ $cm^{-3}$**

# Nanocrystal Conjugate

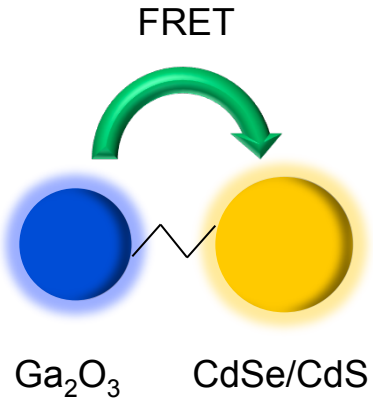


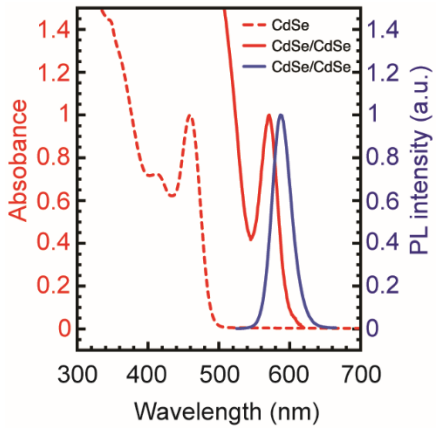


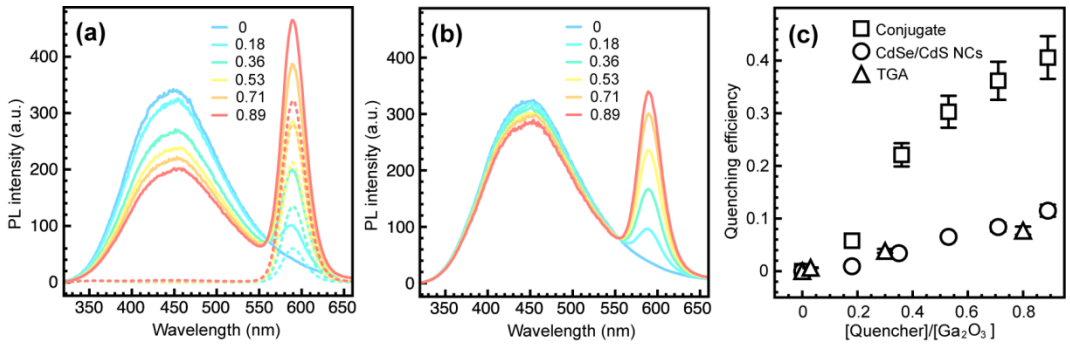


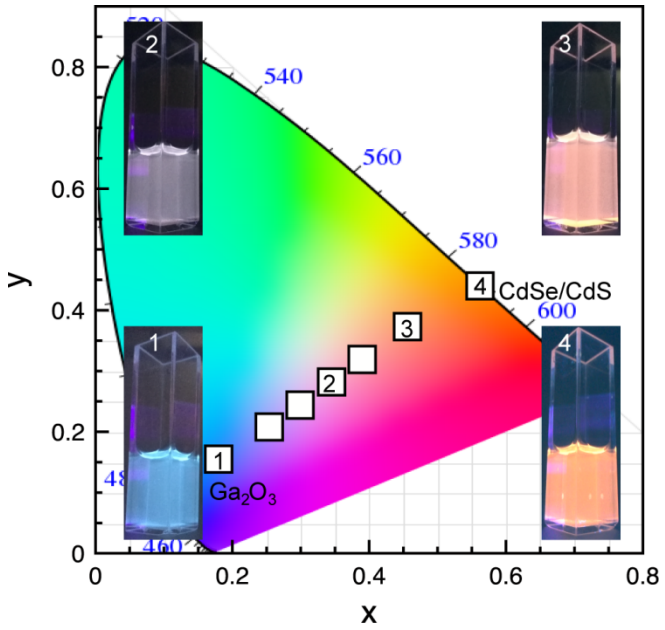


Stanish, P. C.; Radovanovic, P. V. *Nanomaterials*, **2016**, 6, 32

# Johnson-Mehl-Avrami-Kholmogorov (JMAK or KJMA) Model

Andrey Kholmogorov

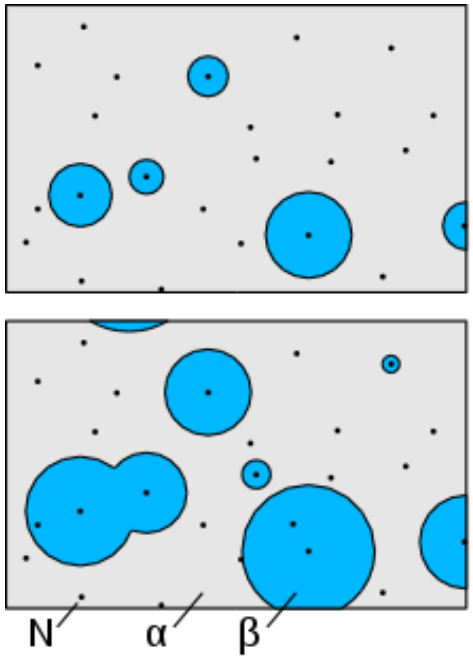


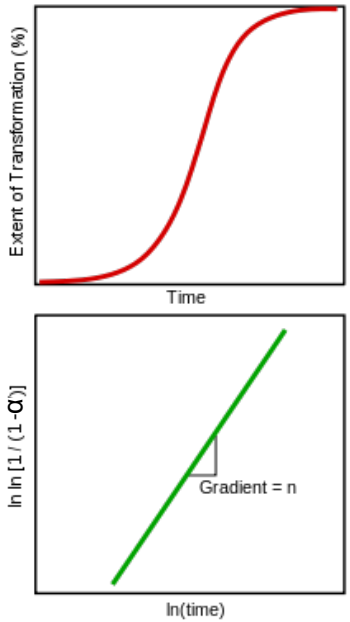


$$-\ln(1-\alpha) = (kt)^n$$

- Nucleation occurs homogeneously over the entire non-transformed material
- The growth rate does not depend on the extent of transformation
- Growth occurs at the same rate in all directions

Avrami, M. *J. Chem. Phys.* **1939**, *7*, 1103–1112.

# Phase Transformation Kinetics

Phase content analysis

$$-\ln(1-\alpha) = (kt)^n$$

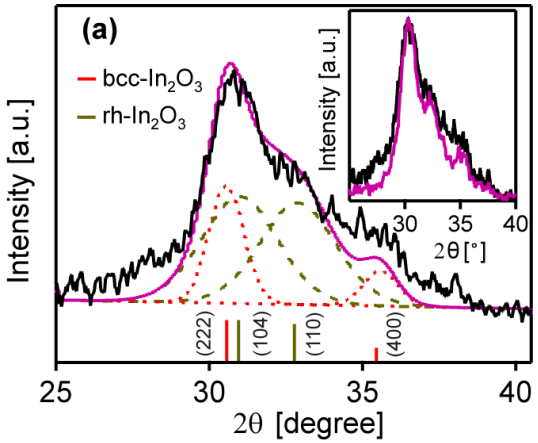


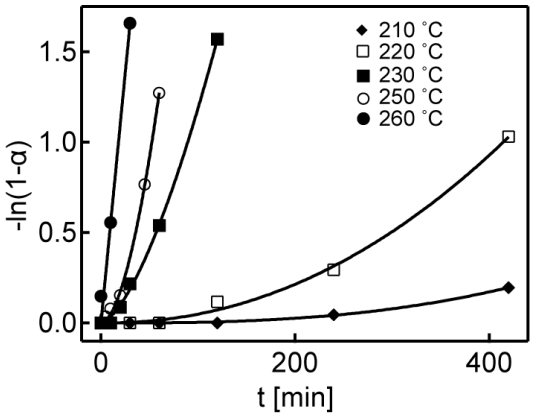


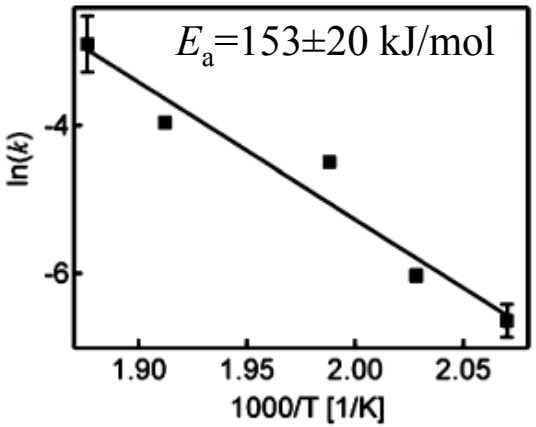


| T (°C) | n | k (min$^{-1}$) |
|---|---|---|
| 210 | 2.6 | 0.0013 |
| 220 | 1.7 | 0.0024 |
| 230 | 1.6 | 0.0112 |
| 250 | 1.4 | 0.0190 |
| 260 | 1.0 | 0.0552 |

$$n = \beta + \lambda/2$$

β -nucleation probability (0-1)

λ – dimensional factor (1, 2, or 3)


Farvid, S. S.; Radovanovic, P. V. *J. Am. Chem. Soc.* **2012**, *134*, 7015-7024.